

Degree project



DETECTION AND ANALYSIS OF *SCLEROTINIA SCLEROTIORUM* IN NATURALLY INFECTED OILSEED RAPE FIELD SAMPLES USING NANOPORE SEQUENCING.

Master Degree Project in Bioscience

Second Cycle 30 credits

Spring term 2024

Student: Tanvi Patil

b19tanpa@student.his.se

Supervisor: Maria Algerin

maria.algerin@his.se

Examiner: Magnus Fagerlind.

magnus.fagerlind@his.se

Abstract

Sclerotinia sclerotiorum, a notorious phytopathogenic fungus, causes sclerotinia stem rot in oilseed rape (*Brassica napus*), a disease with global consequences for oilseed rape productivity and oil quality. The complexity of factors contributing to sclerotinia stem rot makes prediction and control exceedingly challenging. Early and accurate identification of plant pathogens is crucial for effective disease management. This study aimed to establish a method utilizing MinION nanopore sequencing for identifying *S. sclerotiorum* and other fungi causing diseases in oilseed rape. Naturally infected leaf, soil and air samples were collected from oilseed rape fields in Sweden, and DNA was extracted. Two primer pairs targeting the ITS region known marker for fungus identification, were amplified by PCR. For nanopore sequencing, six PCR amplicon samples, two from each source were selected based on their purity and stem rot incidences, with one sample spiked-in with gDNA *S. sclerotiorum* as positive control. Bioinformatic analysis was performed using the CCMetagen tool and EPI2ME. *Ascomycota* and *Basidiomycota* constituted 34% and 45%, respectively, of the identified species. *S. sclerotiorum* was only detected in air field samples, and several other fungal species harmful to oilseed rape production in Sweden, such as *Botrytis cinerea*, *Pyrenopeziza brassicae* and many more, were identified. In conclusion, successful identification of plant pathogens, including *S. sclerotiorum*, was achieved using MinION nanopore sequencer.

Abbreviations

| | |
|---------------|---|
| BP | Base pair |
| CGE | Center for Genomic Epidemiology |
| DNA | Deoxyribonucleic Acid |
| dsDNA | Double-stranded DNA |
| EPI2ME | Epigenetic and Post-Translation Modification in Epigenome |
| gDNA | Genomic DNA |
| ITS | Internal transcribed spacer |
| LSU | Large ribosomal unit |
| MW | Molecular weight |
| NCBI | National Centre or Biotechnology Information |
| NGS | Next-generation sequencing |
| NR | Nuclear ribosomal |
| ONT | Oxford nanopore Technology |
| PCR | Polymerase chain reaction |
| RNA | Ribonucleic acid |
| rRNA | Ribosomal RNA |
| S | Subunit |
| SFB | Short fragmentation buffer |
| SSR | Sclerotinia stem rot |
| SSU | Small sub unit |
| WIMP | What's-in-my-pot |

Popular Scientific Summary

The plant pathogenic fungus *Sclerotinia sclerotiorum* is a common cause of plant disease, affecting a wide range of plants around world. This pathogen is notable for producing black resting structures known as sclerotia and white, feathery growth called mycelium on the infected plants. These features lead to a disease known as sclerotinia stem rot, or white mold, which can harm plants at various growth stages, from young plants to mature ones, and even harvested goods. The fungus typically thrives near the soil and in tissues with high water content.

Infection can happen in two main ways. First, small, hard lumps called sclerotia can grow in the soil and cause infection. Second, mushroom-like structures called apothecia form on the fungus or infected plant debris. These apothecia release tiny spores called ascospores, which can also lead to infection. These ascospores can be carried through the air and settle on healthy plants, causing them to become infected. Such infections lead to significant losses in commercial crops, forcing farmers to use fungicides to prevent the spread. However, to use fungicides effectively and minimize cost, it is essential to assess the levels of infection in the field first. Advanced techniques like polymerase chain reaction (PCR) can help with this assessment. PCR is a lab method that quickly creates millions to billions of copies of a specific DNA region. In this study, PCR was used to target the Internal Transcribed Spacer (ITS) region, a part of DNA within the ribosomal RNA gene cluster of fungi. The ITS region, usually 400 to 900 base pairs long, is a valuable genetic marker for identifying fungi and conducting phylogenetic research. Specific primer pairs, ITS1-ITS2 and ITS1Catta-ITS4ngsUni, were used to target different part of the ITS region. The PCR-amplified DNA fragments were then run through gel electrophoresis alongside a 100-base pair molecular ladder to determine their sizes and confirm successful amplification.

To confirm the presence of *S. sclerotiorum* DNA, genomic DNA (*S. sclerotiorum*) was added to the one of the air samples as a positive control. Six PCR-amplified products were sequenced using MinION nanopore sequencing. The resulting sequences (Fastq files) were analyzed using bioinformatics tools EPI2ME and CCMetagen, revealing the presence of *S. sclerotiorum* in the air samples. Additionally, other fungal species causing plant diseases, including more *Sclerotinia* species, were identified. These belong to the fungal group *Ascomycota* and *Basidiomycota*.

Table of Contents

| | |
|--|----|
| Introduction | 1 |
| Aim..... | 4 |
| Objectives..... | 4 |
| Materials and Methods..... | 5 |
| Biological materials for DNA extraction..... | 5 |
| DNA Extraction from leaves..... | 5 |
| DNA Extraction from soil..... | 5 |
| Extracted DNA from air sample | 5 |
| Measure concentration and purity | 6 |
| PCR and Gel electrophoresis..... | 6 |
| Cleaning of PCR product..... | 7 |
| Extracted <i>Sclerotinia sclerotiorum</i> | 8 |
| Nanopores sequencing (MinION)..... | 8 |
| Library preparation..... | 8 |
| Sequencing | 8 |
| Base calling and analyzing the sequence with bioinformatics database website | 8 |
| Results..... | 9 |
| DNA extraction and cleaning | 9 |
| PCR and Gel electrophoresis (Leaf samples) | 9 |
| PCR and Gel electrophoresis (Pooled leave sample from three field) | 10 |
| PCR and Gel electrophoresis (Soil samples) | 10 |
| PCR and Gel electrophoresis (Air samples) | 11 |
| Measure concentration and purity of cleaned PCR product..... | 11 |
| Minion Sequencing: data analysis | 12 |
| Discussion..... | 15 |
| Conclusion | 19 |
| Ethical aspects and impact on society | 19 |
| Acknowledgement..... | 21 |
| References | 21 |
| Appendices | 29 |

Introduction

The plant fungus *Sclerotinia sclerotiorum* affects a wide range of hosts, including many essential crops such as oilseed rape and soyabean. It is considered to be one of the most severe and most common plant pathogen worldwide, infesting 408 plant species (Jiāng et al., 2013). This fungus thrives in temperate, tropical, and dry environments. *S. sclerotiorum* causes stem rot disease in oilseed rape in Sweden and worldwide (Da Silva Lehner et al., 2017). The disease caused by *S. sclerotiorum* is known by several names, including white mould, watery soft rot, cotton soft rot, bloom blight, and Sclerotinia stem rot, among others. Among these names, "White mould" is a commonly refer to the disease caused by *S. sclerotiorum*. The fungus can invade practically all plant tissues through its mycelia. *S. sclerotiorum* is a highly damaging phytopathogenic fungus, targets plants during the blooming stage of oilseed rape, it can also infect numerous other plants including various vegetable crops, ornamental plants, legumes, and more (Bolton et al., 2005; Derbyshire & Denton-Giles, 2016). The resting structure of *S. sclerotiorum* is capable of remaining in the soil for a long duration as sclerotia. Sclerotia are rigid, black resting body made up of hyphal threads that may remain inactive for lengthy periods of time. Under favorable weather conditions, sclerotia produce apothecia, pale brown fruiting bodies from which ascospores are released into the air (Bolton et al., 2005). Ascospore germination needs a foreign source of nutrients, such as aged plant tissue or pollen. Ascospores are released by the apothecia through carpogenic germination and are the primary source of inoculum for *S. sclerotiorum* infection (Almquist & Wallenhammar, 2014). The disease primarily originates from ascospores falling onto and attaching to petals and leaves, later progressing to infect the stem. The demonstrations of the lifecycle of *S. sclerotiorum* are given in Figure 1. Stem rot incidence measures how frequently stem decay occurs in a group of plants, often caused by fungal or bacterial infections. It indicates the rate at which stem decay develops due to these infections. Factors such as the presence of pathogens, environmental conditions, and agricultural practices all influence its frequency.

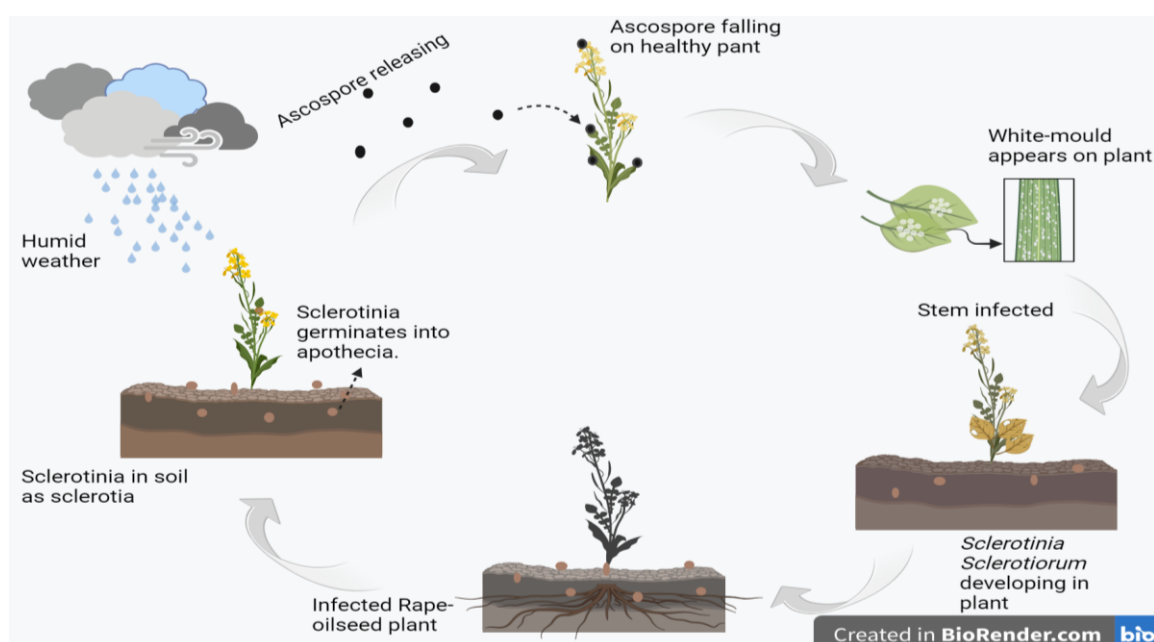


Figure 1. The disease life cycle of *Sclerotinia sclerotiorum* in oilseed rape plants, demonstrating the spread of infection from the initial introduction of sclerotia in the soil to stem penetration and eventual plant death. (Created with Biorender.com).

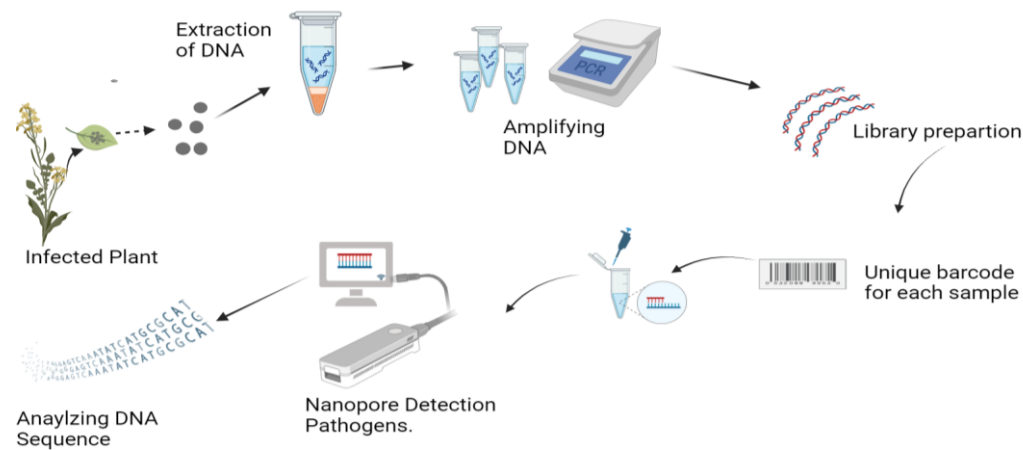
According to Almquist & Wallenhammar (2014), monitoring in agriculture is essential for assessing disease severity and implement control measures. The severity of *Sclerotinia* stem rot is intricately linked to the timing of ascospore release and prevailing meteorological conditions. Managing *S. sclerotiorum* poses significant challenges, particularly due to the absences of disease resistances in oilseed rape. Swedish farmers primarily rely on fungicides application to combat infection, as outlined by Hegedus & Rimmer (2005). However, accurate infection prediction, requires detailed field data, encompassing factors like crop rotation, crop density, previous infection level, and specific weather condition, such as early summer rainfall and flowering period (Twengström et al., 1998; Mei et al., 2010). Despite efforts to improve prediction accuracy, existing model like the SkleroPro model, introduced by German researcher Robert Koch in 2007, have fallen short of expectations (Koch et al., 2007). It was the first model that required minimal data for detecting crop loss and it was dependent on factors such as crop rotation, weather, and the economy. However, the model turned out to be unsatisfactory due to certain drawbacks. One of the drawbacks of the model is its inability to offer precise information on when to apply fungicide or whether fungicide should be used on particular field or not (Koch et al., 2007).

To determine the presence of *S. sclerotiorum* in a specific field, various methods can be used, including both conventional and non-conventional approaches (Almquist & Wallenhammar, 2014). Conventional methods, such as agar plating and soil bioassays are time-consuming and do not provide a measurable indication of infection or assess disease progression before symptoms appear (Baron, 2011). Conversely, non-conventional method offers a rapid, specific, and reliable pathogen evaluation, particularly in the early stages, aiding timely and accurate detection. Techniques like microarray, real-time PCR, and sequencing, identified as less time-consuming alternatives, detecting the presence of desired pathogen in a given sample by utilizing its DNA sequence (Freeman et al., 2002). Molecular-based fungal diagnostic techniques such as DNA sequencing and Polymerase chain reaction (PCR) have revolutionized the molecular diagnosis of pathogenic fungi (Valones et al., 2009). According to Baron (2011), molecular methods offer enhanced sensitivity and specificity, detecting low pathogen levels and minimizing false positives by targeting specific genetic material. Technique like real-time PCR and sequencing yield rapid results, facilitating prompt and improved detection. These methods are crucial for identifying non-culturable pathogens, aiding in the detection of emerging disease and new pathogens. Additionally, they enable efficient high-volume processing, allowing simultaneous analysis of numerous samples with automation reducing labor and time. DNA barcodes are an affordable species-level identification technique that relies on the use of standardized, small parts of the genome called DNA barcodes. The fundamental concept behind a DNA barcode is simple: by sequencing a specific DNA segment (referred to as a barcode) and cross-referencing it with a reference database such as BOLD (Barcode for Life Data System) and the ISHAM (The International Society for Human and Animal Mycology) database, which contains the same DNA portion for known taxonomy. This method is used for referencing a taxonomically unknown species (Hellberg et al., 2016; Irinyi et al., 2015). The ITS region serves as a standard barcode or marker for identifying fungi specimens (Nilsson et al., 2008). The ITS region is flanked by the DNA sequence for ribosomal small subunit (SSU) or 18S subunit at the 5' end and large subunit (LSU) or 28S subunit at 3' end. ITS is further divided into two sections, ITS1 and ITS2, separated by a

5.8S subunit coiled between them (Xu, 2016). The primary factor leading to the widespread use of the ITS barcodes, its notable variability among various fungi. As a result of this advanced approach of ITS, fungal DNA can be directly amplified from complex substrates comprising a variety of DNA origins, such as plant tissue (Gardes & Bruns, 1993).

Nanopore sequencing is a third-generation technique developed by Oxford Nanopore Technologies (ONT) (Lu et al., 2016). The first nanopore sequencer was introduced in 2014, is known as MinION. The MinION device is one of the only portable, real-time instruments for DNA and RNA sequencing (Tyler et al., 2018) It is capable of recognizing lower frequency alleles compared to other NGS generation models as it can sequence a larger area in a single read, including the repeated section (Sun et al., 2022). The development and workings of nanopore sequencing technology have revolutionized the field of genetic analysis. This technique relies on a nanoscale protein that serves as a biosensor, inserted into an electrically resistant polymer membrane. Oxford Nanopore employs flow cells, which are small chambers where DNA samples pass through for analysis, comprising an electro-insulating membrane with a series of small pores known as 'nanopores'. Each nanopore is linked to a corresponding electrode via a channel with a sensor chip, which monitors the electric current passing through the nanopore (Maitra et al., 2012). Molecules, such as DNA or RNA, move through these nanopores. The interruption of the current generates a distinctive "squiggle," indicating the passage of a molecule through a nanopore. Real-time analysis of the squiggle pattern using base-calling techniques enables the determination of the DNA or RNA sequence (Wanunu, 2012).

Sequencing involves three primary steps: library preparation, sequencing, and analysis (see Figure 2). Library preparation is a critical phase where DNA or cDNA fragments are connected to adapters. These adapters, short synthetic DNA strands, facilitate binding of the fragments to the nanopore, a pivotal component of the sequencing machine. Proper attachment of the DNA molecules to the nanopore is ensured through this process. Additionally, adapters can incorporate barcodes, which are unique synthetic DNA sequences, enabling the identification of multiple samples or treatments in a single sequencing run. This capability enhances the efficiency of nanopore sequencing systems, allowing for the processing of numerous samples simultaneously (Zheng et al., 2023). Barcoding involves appending distinct synthetic DNA sequences to DNA fragments, aiding in identifying multiple samples or treatments within flow cells, even if the DNA sequences are identical. The advancement of nanopore technology for sequencing single-long DNA or RNA molecules has led to significant improvements in accuracy, read length, and throughput (Wang et al., 2021; Wanunu, 2012). Nanopore sequencing finds application in various fields, including genotype analysis, single nucleotide polymorphism forensics, whole-genomic sequencing, as well as microbiological detection and taxonomic identification (Wang et al., 2021).



Created in BioRender.com bio

Figure 2: Detailed illustrations of Nanopore sequencing Analyzing DNA sequence to detect pathogens (Created by BioRender.com).

Aim

The main aim of the study was to develop a method to detect *Sclerotinia sclerotiorum* in air, leaf, and soil samples collected from various naturally infected fields in Sweden, using Nanopore sequencing.

Objectives

- DNA extraction from soil and leaves of oilseed rape from fields that are naturally infected by *S. sclerotiorum*.
- Amplification of ITS region from extracted DNA (leaves and soil) using PCR, followed by verifying through Gel electrophoresis. In addition, DNA from previously extracted air samples will also be used to amplify the ITS region by PCR.
- Perform nanopore sequencing to determine whether *S. sclerotiorum* or any other plant pathogens Analysis of the sequences (FASTQ)

Materials and Methods

Biological materials for DNA extraction

This project used biological samples collected from various fields in Sweden, specifically from Dyringe, Skofteby, Forsby, and Kaflas, with respect to the percentage of stem rot incidences. The percentage of infection represents the expected number of plants affected by stem rot disease in each field. These samples comprised naturally infected materials, as specified in Table 1.

Table 1. Presenting biological samples were collected for DNA extraction, with consideration given to incidences of stem rot.

| Samples | Fields | Stem rot incidences (%) |
|---------------|----------|-------------------------|
| Air | Dyringe | 16 |
| Leaf | Skofteby | 25 |
| Leaf and Soil | Forsby | 8 |
| Leaf and Soil | Kaflas | 1 |

DNA Extraction from leaves

To extract DNA from naturally infected oilseed rape leaf, we utilized a modified version of the E.Z.N.A SP Plant DNA Miniprep protocol by Omega Bio-Tek, following the method outlined by Almquist and Wallenhammar (2014). Leaf samples were collected from three fields: Skofteby, Forsby, and Kaflas, each containing ten leaves. Extraction was conducted separately for each field, processing ten leaves at a time. After extracting DNA from individual leaves, the samples from each field were pooled together. Specifically, 5 μ L from each leaf sample within a field were combined to create pooled samples representing their respective fields. The extracted DNA samples were stored at -20°C.

DNA Extraction from soil

DNA extraction from soil samples collected from Forsby and Kaflas field was conducted using the FASTDNA Spin Kit for Soil (MP Biomedical). The protocol was executed by following the manufacturer's instructions, after which the samples were stored at -20°C. The kit is designed for extracting genomic DNA from soil and biological resources including bacteria, fungi, animals, and plants. One samples per field was used for DNA extraction and eluted in 50 μ L nuclease free water.

Extracted DNA from air sample

The provided DNA was extracted from air samples collected using a Burkard spore trap positioned in an oilseed rape field. These samples, gathered on three different dates (6th, 14th, and 16th June 2017), were processed by the supervisor using the Fast DNA Spin Kit (MP Biomedical), following a modified protocol based on Almquist and Wallenhammar (2014). The concentrations are in

Table 2 of the three samples were 0.26 ng/μL for 6th June 2017, 0.36 ng/μL for 14th June 2017, and 0.71 ng/μL for 16th June 2017. The air samples were stored at -20°C.

Measure concentration and purity

The extracted DNA concentrations (leaf and soil), were measured using Invitrogen Qubit 4 fluorometer and the dsDNA HS assay kit from Thermo Fisher Scientific, as well as the DeNovix DS-11+ spectrometer. Furthermore, the purity of the extracted DNA was evaluated by measuring the absorbance ratios $A_{260/280}$ and $A_{260/230}$ using a Nanodrop (DeNovix DS-11+ spectrometer).

PCR and Gel electrophoresis

The primary focus of PCR optimization was on determining the appropriate annealing temperature. Two primer pairs, ITS1Catta-ITS4ngsUni (SIGMA) and ITS1-ITS2 (SIGMA), were employed to cover a large region of ITS. The primer sequences can be found in Table 2. The PCR reaction used the Phusion™ Hot Start II high-fidelity DNA polymerase kit (Thermo Fisher scientific). Various annealing temperatures, calculated to be optimal using NEB Tm calculator (NEB TM Calculator, n.d.) were tested: 61°C to 65°C for primer ITS1-ITS2 and 58°C to 63°C for primer pair ITS1Catta-ITS4ngsUni. DNA from leaf samples from Skofteby field were used for optimization. Subsequently, PCR was run again on three fields, Forsby and Kaflas and Dyringe fields using the optimized temperature of 63°C for primer pair ITS1-ITS2 and 58°C for primer pair ITS1Catta-ITS4ngsUni. The amplification process was carried out using the BIO-RAD IPTC-200 thermal cycler, and a 25 μL PCR mixture with varied in DNA template concentration as specified in Table 3. The PCR cycle, detailed in Table 4, was conducted for 35 cycles for soil, 30 cycles for leaf samples and air samples.

The PCR product was confirmed using 1% agarose gel to observe a band within the 400-700 bp range. Amplicons of 5 μL from PCR were mixed with 1 μL 6X purple gel loading dye (New England Biolabs) and loaded onto a 1% agarose gel in 1X TAE Buffer. A 100 bp molecular weight DNA Purple ladder (New England Biolabs) was loaded into first well as a reference. The gel ran at a voltage of 90-100v for 1 hrs. Visualization was done using 1X gel green, and gel was imaged using imagLab (BioRad) software.

Table 2. Presenting two different primer pairs and their sequences.

| Number | Primers | Sequences | References |
|---------------------|------------|----------------------------|-----------------------------|
| Primer set 1 | ITS1Catta | 5´ ACCWGC GGARGGATCATT A3´ | Tedersoo and Anslan (2019) |
| | ITS4ngsUni | 5´ CCTSCSCTTANTDATATGC3´ | Tedersoo and Lindahl (2016) |
| Primer set 2 | ITS1 | 5´ TCCGTAGGTGAACCTGCGG 3´ | White et al. (1990) |
| | ITS2 | 5´ GCTGCGTTCTTCATCGATGC3´ | White et al. (1990) |

Table 3. Presenting PCR 25µL reaction tube components and their concentration.

| Components | Final concentration | Rxn in 25 µL |
|--|---------------------|-----------------------|
| 5X Phusion HF buffer | 1 X | 5 µL |
| 10mM dNTPs | 200 µM | 0.5 µL |
| 100 µM Primer R | 0.5 µM | 1.25 µL |
| 100 µM Primer F | 0.5 µM | 1.25 µL |
| Template DNA | 1-2 ng/µL | ~2-3 µL |
| Phusion Hot start II DNA polymerase | 0.02U/ µL | 0.25 µL |
| Water | - | Add to make up volume |

Table 4. Presenting PCR cycle for both primer pairs.

| Cycle steps | Temperature | Time | cycles |
|-----------------------------|-------------|------------|--------|
| Initial Denaturation | 98°C | | 1 |
| Denaturation | 98°C | 5-10s | |
| Annealing | | 30s | |
| ITS1 & ITS2 | 63°C | | 30-35 |
| ITS1 Catta & ITS4ngs Uni | 58°C | | |
| Elongation | 72°C | 60s | |
| Extension | 72°C | 10 minutes | 1 |

* Leaf and air samples for 30 cycles and 35 cycle for soil sample.

Cleaning of PCR product

To obtain clean amplicons by eliminating primers, nucleotides, salts, and other interfering elements from the PCR samples, the QIAquick®PCR purification kit (Qiagen) was used, following the manufacturer's instructions. Subsequently, the DNA concentration was measured using a Qubit 4 fluorometer (Thermofisher scientific) with the dsDNA HS assay kit (Thermofisher scientific), and a Nanodrop (DeNovix Ds-11+ spectrometer) (Thermofisher scientific) was used to assess the purity of the samples.

Extracted *Sclerotinia sclerotiorum*

The supervisor provided genomic DNA of *S. sclerotiorum* to serve as a positive control, confirming its presence in the air, leaves, and soil samples. Furthermore, 0.5 ng of gDNA of *S. sclerotiorum* was spiked into one of the air samples.

Nanopores sequencing (MinION)

All instructions were followed from Oxford Nanopore Technologies using a Minion device. The Nanopore sequencing consist of three main steps: library preparation (DNA extracted from three different type of samples), sequencing and base calling and finally, analyzing the sequence with bioinformatics databases.

Library preparation

The amplicons were selected based on concentration and purity, with an absorbance ratio of $A_{260/280}$ and $A_{260/230}$. The required sample amount was 100-200 fmol. Ligation Kit V14 (SQK-LSK114) requirement dictated that the sample should have meet criteria of $A_{260/280} = 1.8$ and $A_{260/230} = 2.0-2.2$. The Native barcoding expansion kit 96 V14 (SQK-NBD114.96) and ligation sequencing kit 96 V14 (SQK-LSK114) was used, following instructions from Oxford Nanopore Technologies. NEBio Calculator (New England Biolabs) was used to determine the exact amount needed for library preparation. A total of six samples were selected, with each set comprising two samples from leaves, soil, and air. Six unique barcodes, NB01-NB06 (A-F), were employed to label six sample in single experiment, prioritizing time and cost efficiency. In order to achieve short fragmentation, the short fragmentation buffer (SFB) was utilized instead of long fragmentation buffer. The SFB helps to sequences DNA fragments of various lengths, guaranteeing precise sequencing and effective library building. The six barcoded samples were pooled together, with a short fragmentation buffer was expected to yield products ranging from of 400-900 base pairs.

Sequencing

The sequencing libraries were sequenced using a FLO-MIN 114 version R 10.4.1 from Oxford Nanopore Technologies. The MinION device (Oxford Nanopore Technologies) was connected to a computer with MinKNOW software, which had already installed in the lab. This setup was maintained at room temperature for around 72 hours at 80-90 volts.

Base calling and analyzing the sequence with bioinformatics database website

The MinKNOW software generates data in Fastq file format, with build-in guppy basecaller covertes MinION POD5 data into Fastq files during automated analysis for sequencing. Subsequently, the Oxford Nanopore workflow agent EPI2ME, a cloud-based data analysis tool, provided by Oxford Nanopore, was used to examine the Fastq files. This examination includes tasks such as quality control, demultiplexing, read alignment, variant identification, gene expression analysis, functional annotation of gene, and generation of visualizations and summary reports for interpretation and presentation. Utilizing the "What's in my pot?" (WIMP) workflow, EPI2ME software facilitated real-time identification of bacteria, fungi, archaea, and viruses through quantitative analysis, a method previously utilized by Juul et al. (2015) for real-time species identifications on MinION. This workflow yielded two reports: a quality control (QC)

report and a WIMP report, displaying the quality of barcoded samples, read size abundance, q-score quality, and pore yield.

Subsequently, the six samples were further analyzed at the Centre for Genomic Epidemiology (CGE), a free-online Bioinformatics server. At CGE, CCMetagen, a recently developed read mapping approach was utilized for uploading the survived Fastq files. CCMetagen (ConClave-based Metagenomic) is a highly accurate metagenomic classification workflow that surpasses other tools in detecting bacteria and fungi.

Results

DNA extraction and cleaning

The concentration and purity ($A_{260/230}$ and $A_{260/280}$) of DNA extracted from leaf and soil sample are provided in Table 5, while detailed information for each sample, field wise is presented in Appendix 1 to Appendix 5.

Table 5. Presenting leaf and soil samples concentration and purity.

| Samples | | Qubit fluorometer ranged (ng/ μ L) | DS-11+spectrometer Concentration ranged (ng/ μ L) | Absorbances | |
|----------------|----------|--|---|---------------|---------------|
| | | | | $A_{260/230}$ | $A_{260/280}$ |
| Leaf | Skofteby | 0.40 to 0.84 | 0.98 to 3.24 | 0.29 to 1.83 | 2.27 to 5.60 |
| | Forsby | 0.30 to 0.85 | 0.56 to 6.48 | 0.30 to 0.61 | 0.47 to 1.82 |
| | Kaflas | 0.80 to 2.38 | 1.31 to 6.39 | 0.31 to 1.16 | 0.56 to 2.60 |
| Pooled leaf | Skofteby | 0.96 | 6.06 | 0.73 | 1.97 |
| | Forsby | 1.37 | 20.12 | 0.65 | 2.58 |
| | Kaflas | 0.65 | 18.42 | 0.64 | 2.44 |
| Soil | Forsby | 0.38 | 18.49 | 0.04 | 2.13 |
| | Kaflas | 0.41 | 6.64 | 0.07 | 1.60 |

PCR and Gel electrophoresis (Leaf samples)

After amplification, PCR-cleaned products were run on agarose gel. Notably, clear bands were observed in samples from primer pair ITS1 and ITS2 at annealing temperatures of 61°C and 62°C, appearing at 400 bp. However, at higher temperatures, specifically 63 °C, 64 °C, and 65 °C, there was good visibility of clear bands, and the observed bands fell within the range of 400-700 bp, see Appendix 6(A). Therefore, an annealing temperature of 63°C was selected as the optimal annealing temperature based on its band clarity. For the primer pair ITS1Catta and ITS4ngs Uni, temperature of 58°C showed a good visibility band between 500-700 bp. However, as the

temperature increased, visibility decreased and weak bands were observed from 59°C to 63°C, see Appendix 6(B). Therefore, an annealing temperature of 58°C was selected the optimal annealing temperature. Subsequently, for further samples from the Forsby and Kaflas fields, the primer pairs were run separately at 63°C for ITS1-ITS2 and 58°C for ITS1Catta-ITS4ngsUni. The gel images for the Forsby and Kaflas fields, featuring primer pairs ITS1-ITS2 and ITS1Catta-ITS4ngs Uni, can be seen in Appendix 7(A and B) respectively.

PCR and Gel electrophoresis (Pooled leaf sample from three field)

All ten samples from each three fields, Skofteby, Forsby and Kaflas, were pooled separately. PCR was rerun for both primer pairs at the optimum temperatures: 58°C for ITS1 Catta- ITS4ngs Uni and 63°C for ITS1-ITS2. The samples were loaded onto agarose gel electrophoresis. With primer pair ITS1-ITS2, the optimized temperature samples from the three fields exhibited bands slightly below 400 bp. However, sample from the three fields using the primer pair ITS1 Catta- ITS4ngs at Uni were between 500-700 bp, as shown in Figure 3.

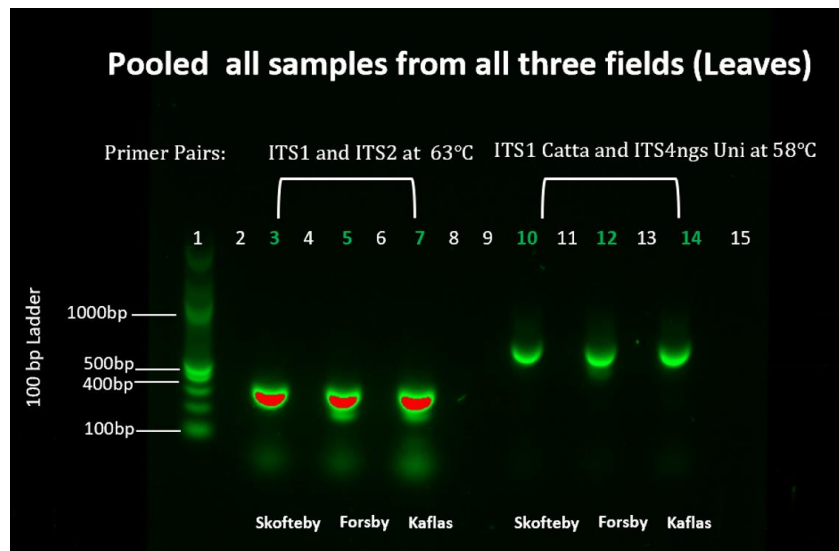


Figure 3: Gel displays PCR-amplified products, which were run using two different primer pairs and temperatures. The primer pair ITS1 and ITS2 was used for samples in lanes 3,5, and 7, with an annealing temperature of 63 °C. For primer pair ITS1 Catta and ITS4ngs Uni, samples were run in lane 10,12, and 14 were run at an annealing temperature of 58 °C. These samples comprised pooled leaf samples from Skofteby, Forsby and Kaflas fields.

PCR and Gel electrophoresis (Soil samples)

The soil samples from the Forsby and Kaflas fields underwent PCR under the same temperatures as the leaf samples: 58°C for primer pair ITS1 Catta- ITS4ngs Uni and 63°C for ITS1-ITS2, although weaker bands were observed for primer pair ITS1-ITS2. However, due to low concentration of DNA template, primer ITS1 Catta – ITS4ngs Uni did not show any bands for the Kaflas field sample, but did exhibit a band for the Forsby field sample. To address this issue, the DNA template concentration was increased to approximately 2 ng for sample from both fields, and PCR was rerun using the primer pair ITS1 Catta and ITS4ngs Uni at gradient temperatures ranging 54°C to 58°C. For the Forsby field, good band visibility was observed at 54°C and 58°C, while fainter bands

were noticeable at 55°C, 56°C and 57°C; thus 58°C was selected as the optimum temperature. However, no bands were observed for the Kaflas field, results can be found in Appendix 8(A). The Kaflas field sample underwent PCR again at a concentration of 4-5 ng in 50 µL, using the primer pair ITS1 Catta and ITS4ngs Uni; unfortunately, no bands were detected. As for primer pair ITS1 and ITS2, the same optimal temperature of 63°C as the leaf sample was used, with only change being an increase in the amount of DNA template (~2 ng). The soil samples from Forsby and Kaflas were rerun for both primer pairs at their optimum temperature, resulting in the observation of bands at 500 bp, can be found in Appendix 8(A & B).

PCR and Gel electrophoresis (Air samples)

The air samples previously extracted by the supervisor were used for PCR analysis. Three samples were collected on June 6th, 14th, and 16th, 2017, from Dyringe field. However, due to low concentration of template DNA, the resulting bands were weak. Therefore, PCR was rerun for both primer pairs at their optimum temperatures: 58°C for ITS1 Catta- ITS4ngs Uni and 63°C for ITS1-ITS2. In this second attempt, the DNA concentration was slightly increased to 2 ng, and the number of cycles was adjusted to 35. Subsequently, the sample were loaded onto 1% agarose gel electrophoresis. The results revealed that samples with the primer pair ITS1-ITS2 displayed good and high-concentration bands in all three sample. In contrast, the primer pair ITS1 Catta-ITS4ngs Uni showed only a band for the sample extracted on June 14th, 2017. No bands were observed for the sample extracted on June 6th, and the bands for sample extracted on June 16th were weak, as shown in Appendix 9(A). Following this, the PCR for ITS1 Catta- ITS4ngs Uni at 58°C was rerun for all three samples can be found in Appendix 9(B).

Measure concentration and purity of cleaned PCR product

Amplicons generated from PCR using primer pairs ITS1-ITS2 and ITS1 Catta-ITS4ngs Uni were subjected to purification and quantification, with their purity being assessed. For subsequent sequencing, only six, most pure samples, indicating by an $A_{260/230}$ ratio between 2.0 and 2.2 and $A_{260/280}$ ratios of 1.8, were selected. Unique barcodes were assigned to each for further identification during sequencing.

Table 6. DNA quantification of six cleaned PCR products and purity results; barcode refers to samples.

| Samples | Primer pairs | Qubit concentration (ng/µL) | Absorbance | | Barcodes |
|--|----------------------|-----------------------------|---------------|---------------|----------|
| | | | $A_{260/230}$ | $A_{260/280}$ | |
| Kaflas (pooled leaf) | ITS1-ITS2 | 6.08 | 1.97 | 1.7 | NB01 |
| Skofteby (pooled leaf) | ITS1Catta-ITS4ngsUni | 7.10 | 1.35 | 2.06 | NB02 |
| Forsby (soil) | ITS1-ITS2 | 5.82 | 1.26 | 1.85 | NB03 |
| Kaflas (soil) | ITS1-ITS2 | 6.36 | 1.50 | 1.87 | NB04 |
| Dyringe (air:16th June 2017) | ITS1-ITS2 | 18.6 | 2.06 | 1.97 | NB05 |

| | | | | | |
|--|----------------------|------|------|------|------|
| Dyringe (air:14th June 2017) | ITS1Catta-ITS4ngsUni | 4.70 | 1.23 | 1.91 | NB06 |
|--|----------------------|------|------|------|------|

Minion Sequencing: data analysis

Two bioinformatics analysis tools, EPI2ME and CCMetagen, were utilized to examine the sequences (Fastq files) generated by MinION sequencing.

EPI2ME (WIMP v2.0)

When utilizing the EPI2ME (WIMP) workflow for analysis, a total of 7,877,096 reads were examined. Out of these 4,039,230 reads were classified based on genomic characteristics, while 3,837,866 were unclassified. The EPI2ME workflow successfully analyzed only 4,039,230 reads out of total. The majority of classified reads belonged to Bacteria (61%) with *Escherichia coli* being the most prevalent, followed by Eukaryota (39%). Viruses and Archaea each comprising less than 1%. *S. sclerotiorum* was not detected by EPI2ME workflow, despite spiking genomic DNA (*S. sclerotiorum*) in air sample as a positive control, in order for detection in other samples. The distribution of reads per the six barcodes can be found in Table 7, and taxonomy report generated classified reads from EPI2ME in Figure 4.

Table 7. Reads counts generated from EPI2ME for all six barcodes.

| Sample | Barcodes | Reads Counts |
|---|-----------|--------------|
| Leaf + spiked with control from kit. | Barcode01 | 1,436,283 |
| Leaf | Barcode02 | 951,665 |
| Soil | Barcode03 | 2,102,913 |
| Soil | Barcode04 | 2,067,459 |
| Air+ Spiked (gDNA) | Barcode05 | 1,202,251 |
| Air | Barcode06 | 116,525 |

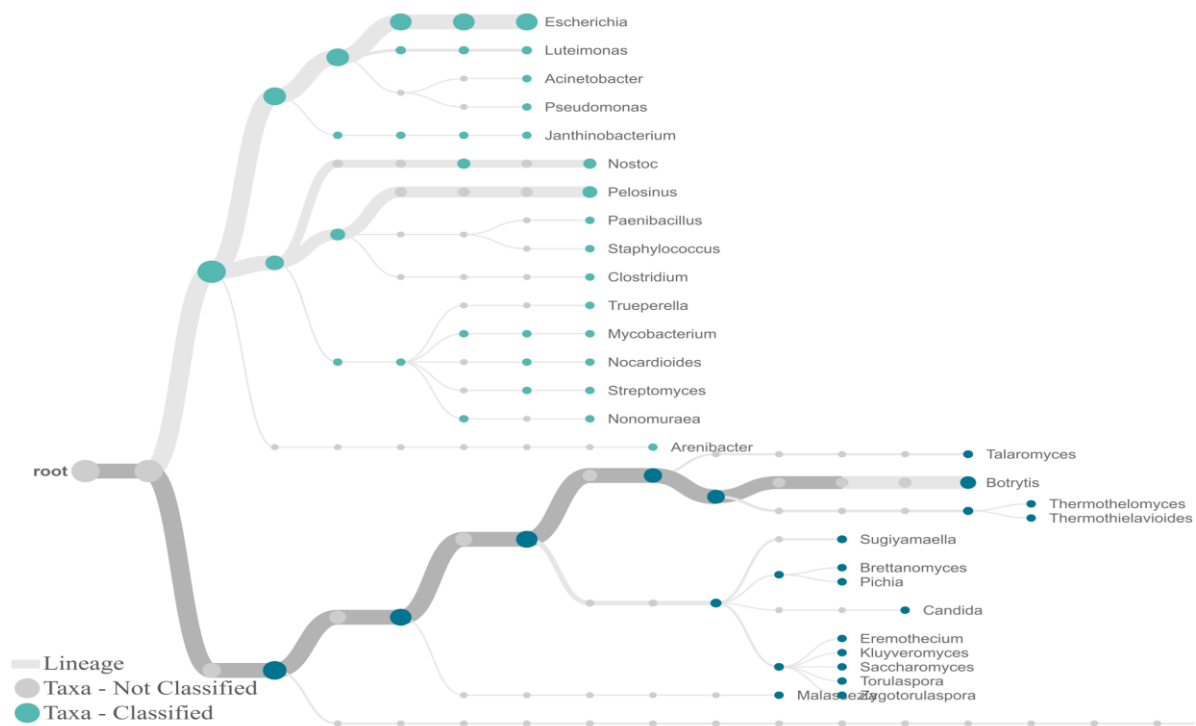


Figure 4. An interactive taxonomy tree visually represents six samples, with larger green dots denoting classified data and grey dots indicating unclassified data. This approach offers a clear and intuitive way to explore the classification status of sample within the broader taxonomic framework.

CCMetagen (ConClave-based Metagenomics v1.2)

CCMetagen, a bioinformatics server from the Centre for Genomic Epidemiology (CGE), generates krona plots for each sample. It successfully detected *Sclerotinia sclerotiorum* from Air samples. In 16th June 2017 air sample, *S. sclerotiorum* is observed at 63% and in 14th June 2017 air sample, it is observed at 12%, as illustrated in Figure 5 and 6. Additionally, the entire Krona plot for 16th June 2017 sample is in Appendix 10 and for 14th June 2017 sample in Appendix 11. However, *S. sclerotiorum* was not observed in the leaf samples (pooled leaf sample from Skofteby and Kafflas) as depicted in Appendix 12 and 13. Similarly, it was not found in Forsby soil and Kafflas soil samples, as shown in Appendix 14 and 15. The server also detected other fungi divisions such as *Ascomycota*, *Basidiomycota*, along with other pathogens belonging to the divisions including *Brassicales*, *Streptophyta*, *Viridiplantae*, which were commonly found across all samples (leaf, soil, and air). The other fungi like *Botrytis cinerea*, *Alternaria alternata*, *Alternaria infectoria*, *Pyrenopeziza brassicae*, *Pythium*, and *Phytophthora* affecting the oilseed rape plant were also detected in different samples and are presented in Appendix 16.

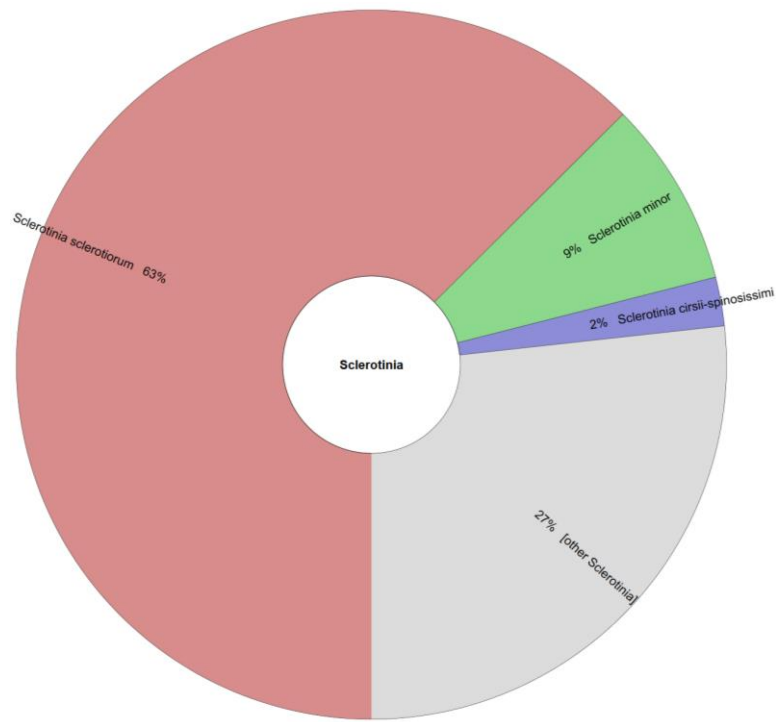


Figure 5. A screenshot of the krona plot generated by CCMetagen for the air sample collected on 16th June 2017, using primer pair ITS1-ITS2. This sample was spiked with gDNA of *S. sclerotiorum*, indicating the presence of *S. sclerotiorum* at level of 63%.



Figure 6. A screenshot of the krona plot generated by CCMetagen for the air sample collected on 14th June 2017, using primer pair ITS1Catta-ITS4ngsUni. Indicating the presence of *S. sclerotiorum* at level of 12%.

Discussion

The study aimed to detect *S. sclerotiorum* in leaf, soil, and air samples from infected oilseed rape fields in Sweden using Oxford Nanopore Technologies' MinION device. This method addresses the challenge of fungal detection in agricultural settings with diverse contamination sources. To achieve this, DNA isolation from leaf, soil and air samples was initiated. Samples were collected from three distinct leaf fields: Skofteby, Forsby and Kaflas, as well as two soil fields: Forsby and Kaflas, and one air field, Dyringe. The isolation process for leaf utilized a modified extraction methodology specifically adapted for the E.Z.N.A.[®] plant DNA kit, describe by Almquist and Wallenhammar (2014) and the FASTDNA Spin Kit for Soil. Air samples had already been proceeded by supervisor using the Fast DNA Spin, following a modified protocol based on Almquist and Wallenhammar (2014). This methodology aimed to extract high-quality DNA suitable for precise quantification.

The quantification process utilized the Qubit dsDNA HS assay kit with the Invitrogen Qubit 4 Fluorometer, known for accurately quantifying DNA from various samples (Panozzo et al., 2023). Qubit assays, employing fluorescent dyes selectively binding to nucleic acids, offer more precise quantification compared to the Nanodrop (DeNovix DS-11+ spectrometer) (Hussing et al., 2018). However, the DeNovix DS-11+ spectrometer may overestimate DNA concentrations, especially in samples with fragmented DNA or impurities, due to its use of the Beer-lambert equation at 260 nm (García-Alegría, 2020). Abela (2023) and Simbolo et al. (2013) also observed higher DNA concentrations with the DeNovix DS-11+, consistent with the findings in Appendix 1-5. Masago et al. (2021) found Nanodrop measurements consistently 3-3.5 times higher than Qubit, regardless of material, highlighting Qubit's accuracy, especially in degraded samples. García-Alegría (2020) emphasized the importance of using both Nanodrop and Qubit for accurate DNA qualification. While Nanodrop is useful for higher concentrations, its reliability for low DNA concentrations, particularly in samples with fragmented DNA or impurities, is uncertain. Therefore, the sequential use of Nanodrop and Qubit enhances the success rate of nanopore library preparation and subsequent sequencing (García-Alegría, 2020).

The purity of extracted DNA was assessed using $A_{260/280}$ and $A_{260/230}$ ratios measured by the DeNovix DS-11+ spectrometer, which detects contaminants such as organic substances or salts. According to Ning et al. (2009), the $A_{260/280}$ ratio measures the absorbance of sample at 260 nm (nucleic acids) and 280 nm (proteins), with a typical ratio around 1.8 indicating pure DNA. Ratios in this study varied from 0.56 to 5.60, suggesting issues; lower ratios imply protein contamination, while higher ones might indicate RNA or other organic molecule contamination (Shim et al., 2010). Pineda-Rodriguez et al. (2023) observed similar results, suggesting inconsistent sample quality due to significant contaminants. The $A_{260/230}$ ratio, ideally between 2.0 and 2.2 for pure samples, measures absorbance at 260 nm and 230 nm, where organic compounds, phenol, carbohydrates, and salt absorb. In this study, $A_{260/230}$ ratios ranged from 0.30 to 1.81, indicating the presence of contaminants affecting nucleic acid purity, aligning with observations by Wilfinger et al. (1997) and Abela (2023). Contamination altering DNA concentration can lead to false negatives, impacting molecular biology investigations (Olson & Morrow, 2012), while low DNA concentrations can skew ratio findings, resulting in lower $A_{260/230}$ ratios (Vogelstein and Gillespie, 1979), highlighting the importance of caution, thorough investigations, and adherence to standard laboratory practices.

Traditional fungal taxonomy methods are being replaced by molecular approaches for enhanced accuracy and reliability. Tedersoo (2017) emphasizes the effectiveness of molecular techniques like DNA barcoding and sequencing, with this study focusing on ITS regions for improved sensitivity and accuracy (Toju et al., 2012). While conventional PCR has limitations in detecting non-target species (Grosdidier et al., 2017), sequencing offers advantages, particularly in identifying specific species like *S. sclerotiorum*. In this study Nanopore sequencing was utilized for accurately sequences fungal DNA from complex substrates like plant tissue, surpassing traditional morphology-based techniques. It reveals additional fungal taxa, enhancing understanding of fungal diversity and interactions, guiding disease control strategies, and deepening knowledge of *S. sclerotiorum* ecology (Ohta et al., 2023).

Two primer pairs, ITS1-ITS2 and ITS1Catta-ITS4ngsUni, targeting ITS regions, were used in this study to amplify fungal DNA from *S. sclerotiorum* in leaf, soil, and air samples, a Dikarya fungus within the *Ascomycota* phylum. Previous studies (Loit et al., 2019; Bellemain et al., 2010; De Beeck et al., 2014) have employed these primer pairs. Bellemain et al. (2010) noted that the ITS1-ITS2 primers amplify *Ascomycetes* and *Basidiomycetes*, as well as non-Dikarya fungi, which can lead to biased results. Runnel et al. (2022) suggested using ITS1Catta-ITS4ngsUni primers, which is more specific to Dikarya fungi, avoiding common intron amplification and enhancing taxonomic resolution and species-level efficiency. Using different primer pairs improves taxonomic resolution and avoids bias in amplifying specific taxonomic groups (Bellemain et al., 2010).

To optimize PCR amplification, the annealing temperature was adjusted using a Skofteby field (Leaf) sample. Gradient temperatures ranging from 61°C to 65°C for ITS1-ITS2 and from 58°C to 63°C for ITS1Catta-ITS4ngsUni were tested for 30 cycles. These temperatures were chosen based on previous year student's research and NEB Tm calculator calculations. The objective was to identify an annealing temperature that produced distinct, well-defined bands between 400-700 base pairs (bp) on agarose gel analysis, as suggested by Kress & Erickson (2012). Gel electrophoresis at 63°C displayed a distinct band for primer pair ITS1-ITS2 (Appendix 6-A), aligning with Siddiq (2023) and differing from Kumar and Shukla's (2005) alternate temperature of 60°C. However, Bellemain et al. (2010) suggested that ITS1-ITS2 primers may have mismatches with target sequences, affecting PCR and resulting in varied amplification outcomes. An annealing temperature of 58°C for primer pair ITS1Catta-ITS4ngsUni was chosen for its brighter band compared to other temperatures (Appendix 6-B). While Loit et al. (2019) used the same primer pair, their study contradicted this temperature, opting for 55°C, whereas Abela (2023) observed visible bands at 58.5°C. Malhotra (1998) suggested that the optimal annealing temperature for ITS1Catta-ITS4ngsUni primers varies depending on the DNA sequence, influenced by factors like polymerase type, buffer composition, and cycling conditions.

Qubit fluorometer measurements showed higher concentrations of the primer pair ITS1-ITS2 compared to ITS1Catta-ITS4ngsUni primer pair across all samples (Data not shown). Bellemain et al. (2010) found that ITS1-ITS2 amplifies non-Dikarya fungi, possibly leading to higher concentration readings due to their effective amplification of ITS regions. Conversely, Runnel et al. (2022) noted that ITS1Catta-ITS4ngsUni targets Dikarya fungal species more specifically, potentially explaining the higher concentration readings observed with ITS1-ITS2. Tegg et al. (2012) recommended using ITS1Catta-ITS4ngsUni for identifying fungal infections in leaf tissue due to its effective amplification of targeted areas of ribosomal DNA. The ITS1/ITSII region,

proposed as the standard DNA barcode for fungi and seed plants (Wang et al., 2014), is widely used in DNA barcoding research.

The optimized annealing temperature set for both primer pairs was used for remaining leaf samples from Forsby and Kaflas fields (Appendix 7). Martin and Rygiewicz (2005) used same primer pairs for leaf samples with same numbers of cycles. The annealing temperature for soil samples from Forsby and Kaflas fields (Appendix 8) remained consistent, but adjustments were made: template DNA was increased by 2 ng, and the number of cycles raised to 35. This aligns with Ellison et al. (2006), who emphasized the need to increase cycle numbers for improved detection sensitivity in low-abundance DNA. Similar adjustments were seen in studies by Alvine (2022), who utilized the same primer pair with a different annealing temperature (55°C), and by Wydro (2022), both studies shared similarities regarding soil samples, as they both aimed to enhance detection sensitivity and obtain sufficient target DNA for downstream analysis. At 63°C, bands for primer pair ITS1-ITS2 were observed in both fields (Appendix 8-B), with double bands likely due to inhibitors present, such as humic substances, phenolic compounds, and polysaccharides. Sidstedt et al. (2020) and Timpano et al. (2020) corroborate these findings, highlighting how inhibitors in soil samples can interfere with PCR, resulting in double bands. Sidstedt et al. (2020) observed similar inhibitors hindering PCR by binding to DNA, while Timpano et al. (2020) suggested that multiple species, heterogeneity, or PCR artifacts could cause double bands in soil samples. With the ITS1Catta-ITS4ngs Uni primer pair, bands appeared only in the Forsby sample, not in the Kaflas sample (Appendix 8-A). Bikos and Mason (2019) noted similar variability in band visibility, attributed to factors like DNA purity, concentration, PCR conditions, primer pairs, or loading dye. The absence of bands in the Kaflas sample may indicate differences in DNA concentration, PCR inhibitors, or DNA extraction efficiency, as suggested by Arbeli and Fuentes (2007) and Wydro (2022). Air samples, previously extracted, were subjected to the same annealing temperature and cycle numbers optimized for both primer pairs as in leaf samples, resulting in clear bands for all three samples (6th, 14th, and 16th June 2017) (Appendix 9). Alvine (2022) used the primer pair ITS1Catta and ITS4ngsUni, while Mbareche et al. (2020) used ITS1-ITS2 for air samples. Primer-dimers, observed in leaf, soil, and air samples, likely resulted from primers with 3'-overlaps sticking together, especially in the presence of DNA (Garafutdinov et al., 2020), consistent with findings by Abela (2023) and Garafutdinov et al. (2020). Bands for ITS1-ITS2 were observed at 400 bp, similar to De Beeck et al. (2014) who observed bands at 430 bp, while Kumar and Shukla (2005) and Siddiq (2023) reported similar bands for ITS1Catta-ITS4ngsUni between 500-700 bp.

In this experiment, PCR-cleaned amplicons were prepared for MinION library creation, with devices running for 72 hours under default parameters. To ensure sequencing accuracy, a Kaflas field leaf sample was spiked with a kit control, and a June 16, 2017 air sample was spiked with *S. sclerotiorum* DNA (Hornung et al., 2019). Six samples were selected based on $A_{260/280}$ and $A_{260/230}$ ratios, following the kit protocol (Table 6). Leavitt et al. (2023) detected *Cladonia perforate* using the same kit. Zhang et al. (2023) demonstrated species-level identification for environmental samples with the ONT R10.4.1 flow cell, supporting this study. Data analysis was conducted using EPI2ME and the Centre for Genomic Epidemiology (CGE).

EPI2ME, Oxford Nanopore's bioinformatics platform, facilitates rapid species identification through its "What's in my pot?" (WIMP) feature (D'Andrea et al., 2020). Despite sample spiking, EPI2ME (WIMP) failed to detect *S. sclerotiorum*, with Bacteria dominating (61%) and Eukaryota (39%), viruses, and Archaea (each <1%) (Figure 4). D'Andrea et al. (2020) noted WIMP's

reliance on the centrifuge database, potentially leading to misclassification of closely related species. D'Andrea et al. (2020) also used EPI2ME to identify fungi on dog skin but failed, despite using controls like *Saccharomyces cerevisiae* and *Cryptococcus neoformans*, highlighting the limitations of morphology-based fungal taxonomy. For better fungal identification, consider sample quality, database completeness, and workflow adherence (Hu et al., 2022). Due to memory issues on university PCs, workflows like EPI2ME Metagenomics, which offer comprehensive microbial community analysis, could not be utilized (Mitchell et al., 2017).

The Centre for Genomic Epidemiology (CGE) employs the CCMetagen server for genomic comparisons, utilizing the whole NCBI nucleotide library as a reference for identifying species with partial genomic data across all biological kingdoms. CCMetagen supports various formats like single-end or paired-end, FastA, FastQ, and Compressed (gzip), streamlining automated microbiome research and seamlessly integrating results into microbial community analysis tools due to its user-friendly interface (Marcelino et al., 2020). CCMetagen generates Krona plots for each sample, aiding taxonomic classification through text or interactive plots using the NCBI taxonomy database facilitating diverse microbial identification, even with distant relatives in reference database (McMurdie & Holmes, 2013; Marcelino et al., 2020).

In this study, CCMetagen successfully identified *S. sclerotiorum* and other pathogens from air samples, with 63% observed on 16th June 2017 (Figure 5) and 12% on 14th June 2017 (Figure 6). However, *S. sclerotiorum* was not detected in leaf and soil samples (Appendix 12-15), despite the presence of *Sclerotiniaceae*, the family to which *S. sclerotiorum* belongs. *Sclerotiniaceae* were identified in all samples (leaf, soil, and air), similar to findings by Lorenzini & Zapparoli (2015), who noted their presence in grape plants without further classification. Abela (2023) found similar results in oilseed rape plants, where *Sclerotiniaceae* were consistently detected. Additionally, *Ascomycota* and *Basidiomycota*, along with other pathogens like *Brassicales*, *Streptophyta*, and *Viridiplantae*, were identified. *Ascomycota* and *Basidiomycota* were the most prevalent phyla in all samples, consistent with Loite et al. (2019).

Harmful fungi were discovered in soil, leaf, and air samples, impacting oilseed rape crops (Appendix 16). These findings parallel Neupane et al.'s (2013) research on similar fungal communities affecting oilseed rape plants. *Botrytis cinerea*, which causes "gray mold" disease, was found in air and leaf samples, leading to stem canker and leaf lesions, consistent with observations by Xue et al. (2019) and Abela (2023). *Alternaria alternata*, responsible for "Alternaria leaf spot," appeared in leaf and air samples, displaying circular lesions with concentric rings, mirroring findings by Siciliano et al. (2017). Similarly, *Alternaria infectoria*, with symptoms resembling *Alternaria alternata*, was detected in leaf samples, aligning with Al-Lami et al.'s (2018) identification of *Alternaria* species in oilseed rape plants, with *Alternaria infectoria* being dominant. *Pyrenopeziza brassicae*, known for "light leaf spot" disease, was also found in leaf samples, in accordance with Gilles et al. (2001). Soil-borne diseases, including "damping off" from *Pythium* species and "Phytophthora rots" linked to *Phytophthora*, were evident in both soil samples, paralleling Legrifi et al.'s (2023) observations where these fungi predominated in the soil.

The detection of *S. sclerotiorum* varied between CCMetagen and EPI2ME (WIMP), showcasing their different capabilities in identifying bacteria and fungi. Both databases detected *Botrytis cinerea*, but only CCMetagen identified *S. sclerotiorum*. This discrepancy may result from differences in reference databases, affecting species diversity, genomic coverage, and annotation

quality. Therefore, assessing database quality is crucial for accurate fungal identification. This study's findings align with Yadav et al. (2022), successfully identifying *Candida auris* fungi on apple using CCMetagen. CCMetagen not only detected the desired fungi but also identified other fungi present in the samples. The findings of Baramidze et al. (2024) using EPI2ME are both contradictory and similar to this study. They differ by detecting *Botrytis cinerea* fungi while not detecting *S. sclerotiorum* fungi, yet both studies identified *Botrytis cinerea* fungi.

Although there was no direct comparison between EPI2ME's WIMP taxonomy and CCMetagen, Marcelino et al. (2020) compared EPI2ME's reference database (Centrifuge) with CCMetagen. Marcelino et al. (2020) evaluated various metagenomic software tools, including Centrifuge, Kraken2, and KrakenUniq, and concluded that CCMetagen was the most accurate and efficient. CCMetagen achieved the highest accuracy and F1 scores for detecting fungal species in simulated metagenomes and metatranscriptomes. This performance establishes CCMetagen as the preferred tool for fungal taxonomy analysis in metagenomic datasets (Marcelino et al., 2020). In a related study, Erlandson et al. (2024) used the MinION sequencer to study soil microbial communities across different crop rotations. Their comparison of bulk soil and sentinel samples revealed both shared and unique microbial taxa. The MinION demonstrated its versatility in studying microbial ecosystems for crop and disease management, effectively detecting bacteria and fungi.

Conclusion

In conclusion, when CCMetagen analysis was performed, the study's use of Minion nanopore sequencing was effective in identifying the target fungus, *S. sclerotiorum*, in the air samples. It is possible that *S. sclerotiorum* pathogen was absent from the leaf and soil samples, indicating probable variation among the samples. Other fungal species with a larger percentage were also found, including member of the phyla *Ascomycota* and *Basidiomycota*. Even though these extra species were discovered, the study's primary goal, identifying *S. sclerotiorum* from oilseed rape samples using nanopore sequencing, was effectively accomplished in one out of three different samples. All things considered, the study highlights the potential and efficacy of nanopore sequencing for targeted pathogen detection.

Ethical aspects and impact on society

It is essential to consider the ethical aspects and potential social impact of the study, even if ethical approval was not required. *Sclerotinia sclerotiorum* is, a plant fungus that infects numerous commercially significant crops, leading to substantial worldwide losses. The primary strategy employed by farmers to protect crops against this pathogen is proactive application of fungicide. However, excessive fungicide use in a field may lead to adverse consequences for surrounding species (including plants, animals, and humans) within an ecosystem. To make agriculture more eco-friendly, fungicides and other chemicals should be used in minimum proportions. Ethical considerations should be considered due to potential unknown consequences associated with fungicides usage.

Achieving an environmentally friendly condition involves the use of DNA detection technique such as Nanopore sequencing. Pathogen identification can be swiftly and effectively accomplished with the assistance of MinION Nanopore sequencing technology utilized in this study. MinION surpasses standard farming methods, including culture and PCR-based procedures. Sequencing

offers advantages like shorter turnaround time, increased sensitivity and capacity to identify numerous infections simultaneously. Thorough research, using this technique will yield insights for developing predictive models for disease control. This approach can assist farmers in making better-informed decisions about fungicides use by facilitating early and accurate detection of fungal diseases. Consequently, this may reduce the risk of overuse and prevent the development of resistance in fungal populations. Avoiding these losses will enable farmers to enhance oilseed rape production and reduce prices by eliminating unnecessary treatments. Furthermore, if fungi are absent in the plant, spraying becomes unnecessary, significantly contributing to environmental preservation.

The planned study may help farmers by offering early forecasts of the presence or absence of fungus in fields, which would have a positive social impact. The present work emphasizes the need for further investigation to enhance and broaden the application of MinION nanopore sequencing consequences for sustainable agriculture and food security. Moreover, the research has the potential to contribute to the advancement of more efficient techniques for identifying and managing fungal infections in crops. Detecting fungal infection in crops using advanced methods can help reduce chemical treatments usage and promote more sustainable farming practices. Both outcomes benefit society by lowering chemical exposure and enhancing food security. The experiment offers insights into overcoming challenges and improving time and resource management for future research.

Future Perspectives

Scientific research methods for identifying phytopathogens have been revolutionized by the MinION Nanopore sequencer, known for its portability, affordability, and real-time data generation. These qualities make it a promising tool for future diagnostic successes. To enhance *S. sclerotiorum* identification, specialized primers could be designed to target unique genomic regions, while improving bioinformatics interpretation entails refining algorithms and analytical techniques for sequencing data analysis, potentially incorporating machine learning for enhanced accuracy and speed.

Optimizing sequencing involves adjusting parameters like DNA extraction, library preparation and sequencing conditions, considering alternative DNA extraction kits and techniques. Experimenting with different primers can enhance assay specificity and sensitivity. Adding *S. sclerotiorum* genomic DNA as a positive control before PCR may be beneficial. Improving bioinformatics analysis can be achieved through advanced algorithms, quality control, and incorporating methods like comparative gene omics and metagenomics assembly for better understanding of identified fungal species. These nanodevices may be able to identify problems with plant health before growers see them. They are able to recognize diseases, respond to unusual circumstance, and start the proper disease management procedures. As a result, these tiny smart devices can function as alert and defense mechanisms. To prevent inconsistencies or misunderstandings, advances in bioinformatics processing of sequencing data are essential. The MinION nanopore sequencer holds the potential to advance phytopathogen diagnostics, boosting accuracy, efficiency, and overall comprehension in the field.

Acknowledgement

I would like to express my sincere gratitude to Maria Algerin, who supervised my thesis, for her unwavering support and guidance throughout this entire process. I am also thankful to Nada Mahmoud, my co-supervisor, for her assistance and support during experimental work. Special appreciation goes to my examiner, Magnus Fagerlind, for providing insightful feedback.

Above all, I want to extend my deepest gratitude to my mother and family; her love and constant support have indispensable throughout my journey.

References

- Abela. (2023). Molecular detection of *Sclerotinia sclerotiorum* from petals of oilseed rape by Nanopore sequencing using MinIon. Simple search. <https://his.diva-portal.org/smash/get/diva2:1823904/FULLTEXT01.pdf>
- Almquist, C., & Wallenhammar, A. (2014). Monitoring of plant and airborne inoculum of *Sclerotinia sclerotiorum* in spring oilseed rape using real-time PCR. *Plant Pathology*, 64(1), 109–118. <https://doi.org/10.1111/ppa.12230>
- Alvine, L. B. (2022). Detection of soil borne pathogens causing pea root rot using minion. DIVA. <https://www.diva-portal.org/smash/record.jsf?pid=diva2%3A1684849&dswid=-6076>
- Al-Lami, H. F. D., You, M. P., & Barbetti, M. J. (2018). Incidence, pathogenicity and diversity of *Alternaria* spp. associated with alternaria leaf spot of canola (*Brassica napus*) in Australia. *Plant Pathology*, 68(3), 492–503. <https://doi.org/10.1111/ppa.12955>
- Arbeli, Z., & Fuentes, C. L. (2007). Improved purification and PCR amplification of DNA from environmental samples. *FEMS Microbiology Letters*, 272(2), 269–275. <https://doi.org/10.1111/j.1574-6968.2007.00764.x>
- Ball, B., Langille, M., & Geddes-McAlister, J. (2020). Fun(gi)omics: Advanced and Diverse Technologies to Explore Emerging Fungal Pathogens and Define Mechanisms of Antifungal Resistance. *MBio*, 11(5). <https://doi.org/10.1128/mbio.01020-20>
- Baramidze, V., Sella, L., Japaridze, T., Abashidze, N., Lamazoshvili, D., Dzotsenidze, N., & Tomashvili, G. (2024). Long amplicon Nanopore sequencing of *Botrytis cinerea* and other fungal species present in infected grapevine leaf samples. *Biology Methods & Protocols*. <https://doi.org/10.1093/biomethods/bpad042>
- Baron, E. J. (2011). Conventional versus Molecular Methods for Pathogen Detection and the Role of Clinical Microbiology in Infection Control. *Journal of Clinical Microbiology*, 49(9_Supplement). <https://doi.org/10.1128/jcm.00807-11>
- Bolton, M. D., Thomma, B. P. H. J., & Nelson, B. D. (2005). *Sclerotinia sclerotiorum* (Lib.) de Bary: biology and molecular traits of a cosmopolitan pathogen. *Molecular Plant Pathology*, 7(1), 1–16. <https://doi.org/10.1111/j.1364-3703.2005.00316.x>

- Bellemain, E., Carlsen, T., Brochmann, C., Coissac, E., Taberlet, P., & Kausserud, H. (2010). ITS as an environmental DNA barcode for fungi: an in silico approach reveals potential PCR biases. *BMC Microbiology*, 10(1), 189. <https://doi.org/10.1186/1471-2180-10-189>
- Bikos, D. A., & Mason, T. G. (2019). Band-collision gel electrophoresis. *Nature Communications*, 10(1). <https://doi.org/10.1038/s41467-019-11438-9>
- Brown, B. L., Watson, M., Minot, S. S., Rivera, M. C., & Franklin, R. B. (2017). MinION™ nanopore sequencing of environmental metagenomes: a synthetic approach. *Gigascience*, 6(3). <https://doi.org/10.1093/gigascience/gix007>
- Bruijns, B., Hoekema, T., Oomens, L., Tiggelaar, R. M., & Gardeniers, H. (2022). Performance of spectrophotometric and fluorometric DNA quantification methods. *Analytica*, 3(3), 371–384. <https://doi.org/10.3390/analytica3030025>
- D'Andreano, S., Cuscó, A., & Francino, O. (2020). Rapid and real-time identification of fungi up to species level with long amplicon nanopore sequencing from clinical samples. *Biology Methods & Protocols*, 6(1). <https://doi.org/10.1093/biomethods/bpaa026>
- Da Silva Lehner, M., De Paula Júnior, T. J., Del Ponte, E. M., Mizubuti, E. S. G., & Pethybridge, S. J. (2017). Independently founded populations of *Sclerotinia sclerotiorum* from a tropical and a temperate region have similar genetic structure. *PLOS ONE*, 12(3), e0173915. <https://doi.org/10.1371/journal.pone.0173915>
- De Beeck, M. O., Lievens, B., Busschaert, P., Declerck, S., Vangronsveld, J., & Colpaert, J. (2014). Comparison and validation of some ITS primer pairs useful for fungal metabarcoding studies. *PLoS One*, 9(6), e97629. <https://doi.org/10.1371/journal.pone.0097629>
- Derbyshire, M. C., & Denton-Giles, M. (2016). The control of *Sclerotinia* stem rot on oilseed rape (*brassica napus*): Current practices and future opportunities. *Plant Pathology*, 65(6), 859–877. <https://doi.org/10.1111/ppa.12517>
- Diaz. (2015). Quantitative detection of *Sclerotinia sclerotiorum* and prediction of stem rot rape seed plant disease by using real time PCR. Simple search. <https://his.diva-portal.org/smash/get/diva2:856350/FULLTEXT02.pdf>
- Ellison, S. L. R., English, C. A., Burns, M. J., & Keer, J. T. (2006). Routes to improving the reliability of low-level DNA analysis using real-time PCR. *BMC Biotechnology*, 6(1). <https://doi.org/10.1186/1472-6750-6-33>
- Erlandson, S. R., Ewing, P. M., Osborne, S. L., & Lehman, R. M. (2024). Sterile sentinels and MinION sequencing capture active soil microbial communities that differentiate crop rotations. *Environmental Microbiome*, 19(1). <https://doi.org/10.1186/s40793-024-00571-8>
- Freeman, J., Ward, E., Calderon, C., & McCartney, A. (2002). *European Journal of Plant Pathology*, 108(9), 877–886. <https://doi.org/10.1023/a:1021216720024>.

- Garafutdinov, R. R., Galimova, A. A., & Sakhabutdinova, A. R. (2020). The influence of quality of primers on the formation of primer dimers in PCR. *Nucleosides, Nucleotides & Nucleic Acids*, 39(9), 1251–1269. <https://doi.org/10.1080/15257770.2020.1803354>
- García-Alegría, A. M., Anduro-Corona, I., Pérez-Martínez, C. J., Guadalupe Corella-Madueño, M. A., Rascón-Durán, M. L., & Astiazaran-García, H. (2020, November 29). Quantification of DNA through the NanoDrop spectrophotometer: Methodological validation using standard reference material and Sprague Dawley rat and human DNA. *International Journal of Analytical Chemistry*. <https://doi.org/10.1155/2020/8896738>
- Gardes, M., & Bruns, T. D. (1993). ITS primers with enhanced specificity for basidiomycetes - application to the identification of mycorrhizae and rusts. *Molecular Ecology*, 2(2), 113–118. <https://doi.org/10.1111/j.1365-294x.1993.tb00005.x>
- Gilles, T., Fitt, B. D. L., McCARTNEY, H. A., Papastamati, K., & Steed, J. M. (2001). The roles of ascospores and conidia of *Pyrenopeziza brassicae* in light leaf spot epidemics on winter oilseed rape (*Brassica napus*) in the UK. *Annals of Applied Biology/Annals of Applied Biology*, 138(2), 141–152. <https://doi.org/10.1111/j.1744-7348.2001.tb00096.x>
- Grosdidier, M., Aguayo, J., Marçais, B., & Ioos, R. (2016). Detection of plant pathogens using real-time PCR: how reliable are late Ct values? *Plant Pathology*, 66(3), 359–367. <https://doi.org/10.1111/ppa.12591>
- Hegedus, Dwayne D., and S. Roger Rimmer. "Sclerotinia Sclerotiorum: When to Be or Not to be a Pathogen?" *FEMS Microbiology Letters*, vol. 251, no. 2, Oct. 2005, pp. 177–184, <https://doi.org/10.1016/j.femsle.2005.07.040>. Accessed 7 Apr. 2022.
- Hellberg, R. S., Pollack, S. J., & Hanner, R. (2016). Seafood species identification using DNA sequencing. In *Elsevier eBooks* (pp. 113–132). <https://doi.org/10.1016/b978-0-12-801592-6.00006-1>
- Hussing, C., Kampmann, M., Mogensen, H. S., Børsting, C., & Morling, N. (2018). Quantification of massively parallel sequencing libraries – a comparative study of eight methods. *Scientific Reports*, 8(1). <https://doi.org/10.1038/s41598-018-19574-w>
- Irinyi, L., Serena, C., Garcia-Hermoso, D., Arabatzis, M., Desnos-Ollivier, M., Vu, D., Cardinali, G., Arthur, I., Normand, A., Giraldo, A., Da Cunha, K. C., Sandoval-Denis, M., Hendrickx, M., Nishikaku, A. S., De Azevedo Melo, A. S., Merseguel, K. B., Khan, A., Rocha, J. a. P., Sampaio, P., . . . Meyer, W. (2015). International Society of Human and Animal Mycology (ISHAM)-ITS reference DNA barcoding database—the quality controlled standard tool for routine identification of human and animal pathogenic fungi. *Medical Mycology*, 53(4), 313–337. <https://doi.org/10.1093/mmy/myv008>
- Jiāng, D., Fù, Y., Li, G., & Ghabrial, S. A. (2013). Viruses of the Plant Pathogenic Fungus *Sclerotinia sclerotiorum*. In *Advances in Virus Research* (pp. 215–248). <https://doi.org/10.1016/b978-0-12-394315-6.00008-8>

- Juul, S., Izquierdo, F., Hurst, A. M., Dai, X., Wright, A., Kulesha, E., Pettett, R., & Turner, D. J. (2015). What's in my pot? Real-time species identification on the MinION. *bioRxiv (Cold Spring Harbor Laboratory)*. <https://doi.org/10.1101/030742>
- Koch, S., Dunker, S., Kleinhenz, B., Röhrig, M., & Von Tiedemann, A. (2007). A Crop Loss-Related Forecasting model for sclerotinia Stem rot in winter oilseed rape. *Phytopathology*, 97(9), 1186–1194. <https://doi.org/10.1094/phyto-97-9-1186>
- Kress, W. J., & Erickson, D. L. (2012). DNA barcodes: methods and protocols (pp. 3-8). Humana Press.
- Kumar, M., & Shukla, P. K. (2005). Use of PCR targeting of internal transcribed spacer regions and Single-Stranded conformation polymorphism analysis of sequence variation in different regions of RRNA genes in fungi for rapid diagnosis of mycotic keratitis. *Journal of Clinical Microbiology*, 43(2), 662–668. <https://doi.org/10.1128/jcm.43.2.662-668.2005>
- Leavitt, S. D., DeBolt, A., McQuhae, E., & Allen, J. L. (2023). Genomic Resources for the First Federally Endangered Lichen: The Florida Perforate Cladonia (*Cladonia perforata*). *Journal of Fungi*, 9(7), 698. <https://doi.org/10.3390/jof9070698>
- Legrifi, I., Taoussi, M., Figuigui, J. A., Lazraq, A., Hussain, T., & Lahlali, R. (2023). Oomycetes Root Rot Caused by *Pythium* spp. and *Phytophthora* spp.: Host Range, Detection, and Management Strategies, Special Case of Olive Trees. *Journal of Crop Health/Journal of Crop Health*, 76(1), 19–47. <https://doi.org/10.1007/s10343-023-00946-w>
- Lin, B., Hui, J., & Mao, H. (2021). Nanopore Technology and its applications in gene sequencing. *Biosensors*, 11(7), 214. <https://doi.org/10.3390/bios11070214>
- Loit, K., Adamson, K., Bahram, M., Puusepp, R., Anslan, S., Kiiker, R., Drenkhan, R., & Tedersoo, L. (2019). Relative Performance of MinION (Oxford Nanopore Technologies) versus Sequel (Pacific Biosciences) Third-Generation Sequencing Instruments in Identification of Agricultural and Forest Fungal Pathogens. *Applied and Environmental Microbiology*, 85(21). <https://doi.org/10.1128/aem.01368-19>
- Lorenzini, M., & Zapparoli, G. (2015). Description of a taxonomically undefined Sclerotiniaceae strain from withered rotten-grapes. *Antonie Van Leeuwenhoek*, 109(2), 197–205. <https://doi.org/10.1007/s10482-015-0621-11>
- Lu, H., Giordano, F., & Ning, Z. (2016). Oxford Nanopore MinION Sequencing and Genome Assembly. *Genomics, Proteomics & Bioinformatics*, 14(5), 265–279. <https://doi.org/10.1016/j.gpb.2016.05.004>
- Maitra, R. D., Kim, J., & Dunbar, W. B. (2012). Recent advances in nanopore sequencing. *Electrophoresis*, 33(23), 3418–3428. <https://doi.org/10.1002/elps.201200272>

- Malhotra, K. (1998). Interaction and effect of annealing temperature on primers used in differential display RT-PCR. *Nucleic Acids Research*, 26(3), 854–856. <https://doi.org/10.1093/nar/26.3.854>
- Marcelino, V. R., Clausen, P. T. L. C., Buchmann, J. P., Wille, M., Iredell, J. R., Meyer, W., Lund, O., Sorrell, T. C., & Holmes, E. C. (2020). CCMetagen: comprehensive and accurate identification of eukaryotes and prokaryotes in metagenomic data. *Genome Biology*, 21(1). <https://doi.org/10.1186/s13059-020-02014-2>
- Martin, K. J., & Rygiewicz, P. T. (2005). Fungal-specific PCR primers developed for analysis of the ITS region of environmental DNA extracts. *BMC Microbiology*, 5(1), 28. <https://doi.org/10.1186/1471-2180-5-28>
- Mbareche, H., Veillette, M., Bilodeau, G., & Duchaine, C. (2020). Comparison of the performance of ITS1 and ITS2 as barcodes in amplicon-based sequencing of bioaerosols. *PeerJ*, 8, e8523. <https://doi.org/10.7717/peerj.8523>
- McMurdie, P. J., & Holmes, S. (2013). phyloseq: An R Package for Reproducible Interactive Analysis and Graphics of Microbiome Census Data. *PloS One*, 8(4), e61217. <https://doi.org/10.1371/journal.pone.0061217>.
- Mei, J., Qian, L., Disi, J. O., Yang, X., Li, Q., Li, J., Frauen, M., Cai, D., & Qian, W. (2010). Identification of resistant sources against *Sclerotinia sclerotiorum* in Brassica species with emphasis on *B. oleracea*. *Euphytica*, 177(3), 393–399. <https://doi.org/10.1007/s10681-010-0274-0>
- Mitchell, A. L., Scheremetjew, M., Denise, H., Potter, S., Tarkowska, A., Qureshi, M., Salazar, G., Pesseat, S., Boland, M., Hunter, F., Hoopen, P. T., Alako, B. T. F., Amid, C., Wilkinson, D. J., Curtis, T. P., Cochrane, G., & Bateman, A. (2017). EBI Metagenomics in 2017: enriching the analysis of microbial communities, from sequence reads to assemblies. *Nucleic Acids Research*, 46(D1), D726–D735. <https://doi.org/10.1093/nar/gkx967>
- Morrison, G. A., Fu, J., Lee, G. C., Wiederhold, N. P., Cañete-Gibas, C. F., Bunnik, E. M., & Wickes, B. L. (2020). Nanopore sequencing of the fungal intergenic spacer sequence as a potential rapid diagnostic assay. *Journal of Clinical Microbiology*, 58(12). <https://doi.org/10.1128/jcm.01972-20>
- Nilsson, R. H., Kristiansson, E., Ryberg, M., Hallenberg, N., & Larsson, K. . (2008). Intraspecific ITS variability in the kingdom fungi as expressed in the international sequence databases and its implications for molecular species identification. *Evolutionary Bioinformatics*, 4, EBO.S653. <https://doi.org/10.4137/ebo.s653>
- Ning, J., Liebich, J., Kästner, M., Zhou, J., Schäffer, A., & Burauel, P. (2009). Different influences of DNA purity indices and quantity on PCR-based DGGE and functional gene microarray in soil microbial community study. *Applied Microbiology and Biotechnology*, 82(5), 983–993. <https://doi.org/10.1007/s00253-009-1912-0>

- Ohta, A., Nishi, K., Hirota, K., & Matsuo, Y. (2023). Using nanopore sequencing to identify fungi from clinical samples with high phylogenetic resolution. *Scientific Reports*, 13(1). <https://doi.org/10.1038/s41598-023-37016-0>
- Olson, N. D., & Morrow, J. B. (2012). DNA extract characterization process for microbial detection methods development and validation. *BMC Research Notes*, 5(1). <https://doi.org/10.1186/1756-0500-5-668>
- Panozzo, A., Barion, G., Moore, S. A., Cobalchin, F., Di Stefano, A., Sella, L., & Vamerali, T. (2023). Early morpho-physiological response of oilseed rape under seed applied Sedaxane fungicide and *Rhizoctonia solani* pressure. *Frontiers in Plant Science*, 14. <https://doi.org/10.3389/fpls.2023.1130825>
- Pineda-Rodriguez, Y. Y., Pompelli, M. F., Jarma-Orozco, A., Rodríguez, N. V., & Rodríguez-Paez, L. A. (2023). A New and Profitable Protocol to DNA Extraction in *Limnospira maxima*. *Methods and Protocols*, 6(4), 62. <https://doi.org/10.3390/mps6040062>
- Runnel, K., Abarenkov, K., Copoț, O., Mikryukov, V., Kõljalg, U., Saar, I., & Tedersoo, L. (2022). DNA barcoding of fungal specimens using long-read high-throughput sequencing. *bioRxiv* (Cold Spring Harbor Laboratory). <https://doi.org/10.1101/2022.02.08.479507>
- Schoch, C. L., Seifert, K. A., Huhndorf, S. M., Robert, V., Spouge, J. L., Lévesque, C. A., Chen, W., Bolchacova, E., Voigt, K., Crous, P. W., Miller, A. N., Wingfield, M. J., Aime, M. C., An, K., Bai, F., Barreto, R. W., Begerow, D., Bergeron, M., Blackwell, M., . . . Schindel, D. E. (2012). Nuclear ribosomal internal transcribed spacer (ITS) region as a universal DNA barcode marker for Fungi. *Proceedings of the National Academy of Sciences of the United States of America*, 109(16), 6241–6246. <https://doi.org/10.1073/pnas.1117018109>
- Shim, S., Kim, J., Jung, S., Kim, D., Oh, J., Han, B., & Jeon, J. (2010). Multilaboratory assessment of variations in Spectrophotometry-Based DNA quantity and purity indexes. *Biopreservation and Biobanking*, 8(4), 187–192. <https://doi.org/10.1089/bio.2010.0016>
- Siciliano, I., Gilardi, G., Ortu, G., Gisi, U., Gullino, M. L., & Garibaldi, A. (2017). Identification and characterization of *Alternaria* species causing leaf spot on cabbage, cauliflower, wild and cultivated rocket by using molecular and morphological features and mycotoxin production. *European Journal of Plant Pathology*, 149(2), 401–413. <https://doi.org/10.1007/s10658-017-1190-0>
- Siddiq. (2023). Analysing rapeseed leaves from naturally infested fields in Skaraborg to detect *Sclerotinia sclerotiorum* using Nanopore sequencing. Simple search. <https://his.diva-portal.org/smash/get/diva2:1779583/FULLTEXT01.pdf>
- Sidstedt, M., Rådström, P., & Hedman, J. (2020). PCR inhibition in qPCR, dPCR and MPS—mechanisms and solutions. *Analytical and Bioanalytical Chemistry*/Analytical & Bioanalytical Chemistry, 412(9), 2009–2023. <https://doi.org/10.1007/s00216-020-02490-2>

- Simbolo, M., Gottardi, M., Corbo, V., Fassan, M., Mafficini, A., Malpeli, G., Lawlor, R. T., & Scarpa, A. (2013). DNA qualification workflow for next generation sequencing of histopathological samples. *PloS One*, 8(6), e62692. <https://doi.org/10.1371/journal.pone.0062692>
- Simon Oxley, & Andy Evans. (2009, June). Winter oilseed rape pest and disease. SRUC. <https://www.sruc.ac.uk/media/yl5da433/tn620-winter-osr.pdf>
- Smith, D., Kermode, A., Cafà, G., Buddie, A. G., Caine, T. S., & Ryan, M. J. (2020). Strengthening mycology research through coordinated access to microbial culture collection strains. *CABI Agriculture and Bioscience*, 1(1). <https://doi.org/10.1186/s43170-020-00004-9>
- Sun, K., Liu, Y., Zhou, X., Yin, C., Zhang, P., Yang, Q., Mao, L., Shentu, X., & Yu, X. (2022). Nanopore sequencing technology and its application in plant virus diagnostics. *Frontiers in Microbiology*, 13. <https://doi.org/10.3389/fmicb.2022.939666>
- Tedersoo, L., & Lindahl, B. (2016). Fungal identification biases in microbiome projects. *Environmental Microbiology Reports*, 8(5), 774–779. <https://doi.org/10.1111/1758-2229.12438>
- Tedersoo, L. (Ed.). (2017). *Biogeography of mycorrhizal symbiosis* (Vol. 230). Cham: Springer.
- Tedersoo, L., & Anslan, S. (2019). Towards PacBio-based pan-eukaryote metabarcoding using full-length ITS sequences. *Environmental Microbiology Reports*, 11(5), 659–668. <https://doi.org/10.1111/1758-2229.12776>
- Tegg, R. S., Thangavel, T., Aminian, H., & Wilson, C. R. (2012). Somaclonal selection in potato for resistance to common scab provides concurrent resistance to powdery scab. *Plant Pathology*, 62(4), 922–931. <https://doi.org/10.1111/j.1365-3059.2012.02698.x>
- Timpano, E. K., Scheible, M. K. R., & Meiklejohn, K. A. (2020). Optimization of the second internal transcribed spacer (ITS2) for characterizing land plants from soil. *PloS One*, 15(4), e0231436. <https://doi.org/10.1371/journal.pone.0231436>
- Toju, H., Tanabe, A. S., Yamamoto, S., & Sato, H. (2012). High-Coverage ITS primers for the DNA-Based identification of ascomycetes and basidiomycetes in environmental samples. *PloS One*, 7(7), e40863. <https://doi.org/10.1371/journal.pone.0040863>
- Twengström, E., Sigvald, R., Svensson, C., & Yuen, J. (1998). Forecasting Sclerotinia stem rot in spring sown oilseed rape. *Crop Protection*, 17(5), 405–411. [https://doi.org/10.1016/s0261-2194\(98\)00035-0](https://doi.org/10.1016/s0261-2194(98)00035-0)
- Tyler, A. D., Mataseje, L., Urfano, C. J., Schmidt, L., Antonation, K. S., Mulvey, M. R., & Corbett, C. R. (2018). Evaluation of Oxford Nanopore's MinION sequencing device for microbial whole genome sequencing applications. *Scientific Reports*, 8(1). <https://doi.org/10.1038/s41598-018-29334-5>

- Vaidya, J. D., Van Den Bogert, B., Edwards, J. E., Boekhorst, J., Van Gastelen, S., Saccenti, E., Plugge, C. M., & Smidt, H. (2018). The Effect of DNA Extraction Methods on Observed Microbial Communities from Fibrous and Liquid Rumen Fractions of Dairy Cows. *Frontiers in Microbiology*, 9. <https://doi.org/10.3389/fmicb.2018.00092>
- Valones, M. a. A., Guimarães, R. L., Brandão, L. a. C., De Souza, P. R. E., De Albuquerque Tavares Carvalho, A., & Crovela, S. (2009). Principles and applications of polymerase chain reaction in medical diagnostic fields: a review. *Brazilian Journal of Microbiology*, 40(1), 1–11. <https://doi.org/10.1590/s1517-83822009000100001>
- Vogelstein, B., & Gillespie, D. (1979). Preparative and analytical purification of DNA from agarose. *Proceedings of the National Academy of Sciences of the United States of America*, 76(2), 615–619. <https://doi.org/10.1073/pnas.76.2.615>
- Wang, Y., Zhao, Y., Bollas, A., Wang, Y., & Au, K. F. (2021). Nanopore sequencing technology, bioinformatics and applications. *Nature Biotechnology*, 39(11), 1348–1365. <https://doi.org/10.1038/s41587-021-01108-x>
- Wang, X., Liu, C., Huang, L., Bengtsson-Palme, J., Chen, H., Zhang, J., Cai, D., & Li, J. (2014). ITS1: a DNA barcode better than ITS2 in eukaryotes? *Molecular Ecology Resources*, 15(3), 573–586. <https://doi.org/10.1111/1755-0998.12325>
- Wanunu, M. (2012). Nanopores: A journey towards DNA sequencing. *Physics of Life Reviews*, 9(2), 125–158. <https://doi.org/10.1016/j.plrev.2012.05.010>
- White, T. J., Bruns, T., Lee, S. J. W. T., & Taylor, J. (1990). Amplification and direct sequencing of fungal ribosomal RNA genes for phylogenetics. *PCR protocols: a guide to methods and applications*, 18(1), 315–322.
- Wilfinger, W. W., Mackey, K., & Chomczynski, P. (1997). Effect of pH and ionic strength on the spectrophotometric assessment of nucleic acid purity. *Biotechniques/BioTechniques*, 22(3), 474–481. <https://doi.org/10.2144/97223st01>
- Wydro, U. (2022). Soil microbiome study based on DNA extraction: a review. *Water*, 14(24), 3999. <https://doi.org/10.3390/w14243999>
- Xu, J. (2016b). Fungal DNA barcoding. *Genome*, 59(11), 913–932. <https://doi.org/10.1139/gen-2016-0046>
- Xue, L. H., Liu, Y., Zhang, L., Huang, X. Q., Zhou, X. Q., Yang, X. X., & Wu, W. X. (2019). Botrytis pseudocinerea, a New Pathogen Causing Gray Mold on Brassica napus in China. *Plant Disease*, 103(2), 367. <https://doi.org/10.1094/pdis-04-18-0688-pdn>
- Yadav, A., Jain, K., Wang, Y., Pawar, K., Kaur, H., Sharma, K. K., Tripathy, V., Singh, A., Xu, J., & Chowdhary, A. (2022). Candida auris on Apples: Diversity and Clinical Significance. *MBio*, 13(2). <https://doi.org/10.1128/mbio.00518-22>

Zhang, T., Li, H., Ma, S., Cao, J., Liao, H., Huang, Q., & Chen, W. (2023). The newest Oxford Nanopore R10.4.1 full-length 16S rRNA sequencing enables the accurate resolution of species-level microbial community profiling. *Applied and Environmental Microbiology*, 89(10). <https://doi.org/10.1128/aem.00605-23>

Zheng, P., Zhou, C., Ding, Y., Liu, B., Lu, L., Zhu, F., & Duan, S. (2023). Nanopore sequencing technology and its applications. *MedComm*, 4(4). <https://doi.org/10.1002/mco2.316>

Appendices

Appendix 1. Concentration and purity of Skofteby field leave samples.

| Sample | Qubit concentration ng/μl | Absorbance 260/230 | Absorbance 260/280 | DS-11+spectrometer Concentration ng/μl |
|--------|---------------------------|--------------------|--------------------|--|
| 1 | 0.78 | 1.27 | 2.50 | 4.496 |
| 2 | 0.84 | 1.83 | 2.27 | 18.245 |
| 3 | 0.28 | 0.29 | 3.07 | 2.826 |
| 4 | 0.74 | 0.42 | 2.23 | 9.953 |
| 5 | 0.22 | 0.44 | -126.25 | 1.025 |
| 6 | 0.50 | 0.73 | 2.25 | 4.752 |
| 7 | 0.39 | 1.49 | 5.60 | 3.752 |
| 8 | 0.71 | 0.92 | 5.21 | 3.977 |
| 9 | 0.45 | 0.38 | 4.13 | 2.125 |
| 10 | 0.43 | 0.41 | -3.68 | 1.441 |

Appendix 2. Concentration and purity of Forsby field leave samples.

| Sample | Qubit concentration ng/μl | Absorbance 260/230 | Absorbance 260/280 | DS-11+spectrometer Concentration ng/μl |
|--------|---------------------------|--------------------|--------------------|--|
| 1 | 0.71 | 0.33 | 1.59 | 1.703 |
| 2 | 1.15 | 0.32 | 1.40 | 1.314 |
| 3 | 2.12 | 0.38 | 1.24 | 1.709 |
| 4 | 0.93 | 0.43 | 0.47 | 1.861 |
| 5 | 1.41 | 0.60 | 1.63 | 4.101 |

| | | | | |
|-----------|-----------------------------|------|------|-------|
| 6 | 1.60 | 0.61 | 1.19 | 1.763 |
| 7 | 0.85 | 0.52 | 1.66 | 6.396 |
| 8 | Sample out of range too low | 0.40 | 1.48 | 2.420 |
| 9 | 1.06 | 0.61 | 1.79 | 4.859 |
| 10 | 2.38 | 0.57 | 1.82 | 5.325 |

Appendix 3. Concentration and purity of Kaflas field leave samples

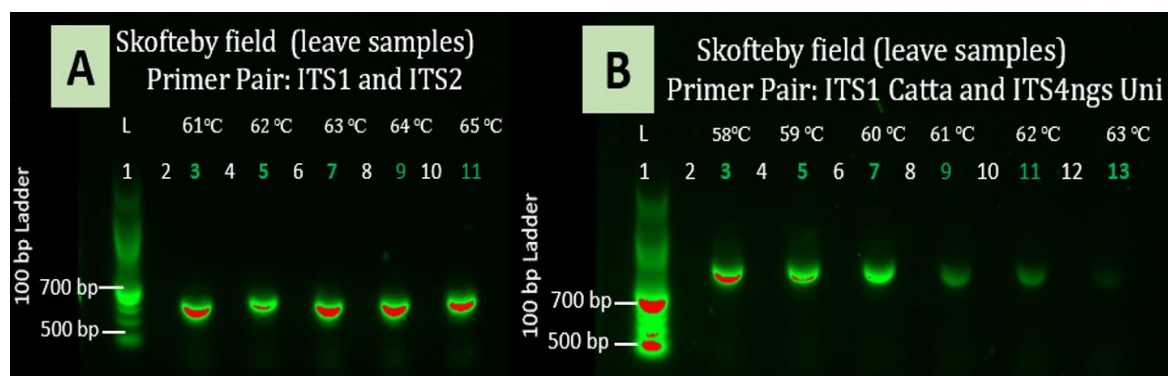
| Sample | Qubit concentration ng/μl | Absorbance 260/230 | Absorbance 260/280 | DS-11+spectrometer Concentration ng/μl |
|---------------|----------------------------------|---------------------------|---------------------------|---|
| 1 | 0.73 | 0.31 | 1.52 | 1.898 |
| 2 | 0.64 | 1.16 | 0.52 | 0.565 |
| 3 | 0.43 | 0.64 | 6.21 | 0.796 |
| 4 | 0.70 | 0.58 | 2.19 | 1.334 |
| 5 | 0.85 | 0.77 | 2.60 | 1.821 |
| 6 | 0.79 | 0.64 | 1.98 | 1.947 |
| 7 | 0.54 | 0.65 | 2.10 | 2.596 |
| 8 | 0.46 | 0.50 | 1.71 | 6.480 |
| 9 | 0.53 | 0.47 | 2.37 | 5.433 |
| 10 | 0.30 | 0.51 | 1.38 | 1.913 |

Appendix 4. Concentration and purity of 10 pooled samples (leaves) from Skofteby, Forsby and Kaflas fields.

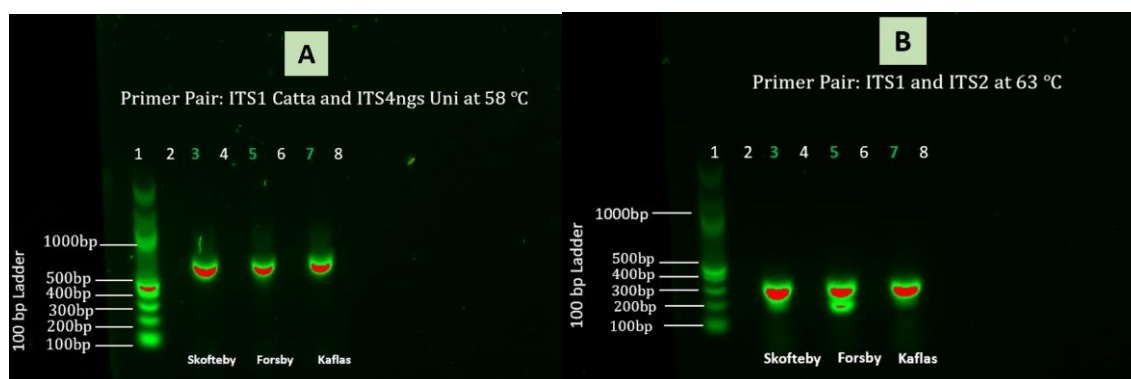
| Sample | Qubit concentration ng/μl | Absorbance 260/230 | Absorbance 260/280 | DS-11+spectrometer Concentration ng/μl |
|-----------------|----------------------------------|---------------------------|---------------------------|---|
| Skofteby | 0.964 | 0.73 | 1.97 | 6.066 |
| Kaflas | 0.650 | 0.65 | 2.58 | 18.425 |
| Forsby | 1.37 | 0.64 | 2.44 | 20.125 |

Appendix 5. Concentration and purity of Kaflas and Forsby fields soil samples per one field.

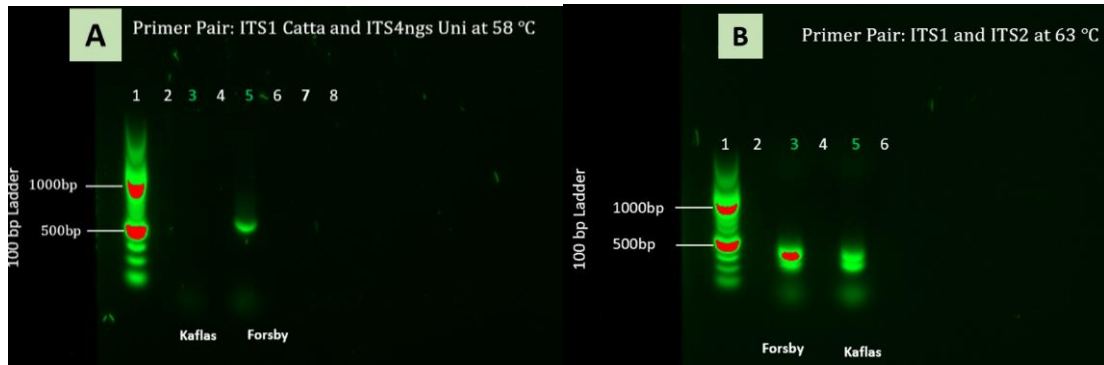
| Sample | Qubit concentration ng/μl | Absorbance 260/230 | Absorbance 260/280 | DS-11+spectrometer Concentration ng/μl |
|--------|---------------------------|--------------------|--------------------|--|
| Kaflas | 0.41 | 0.04 | 2.13 | 6.648 |
| Forsby | 0.38 | 0.07 | 1.60 | 18.495 |



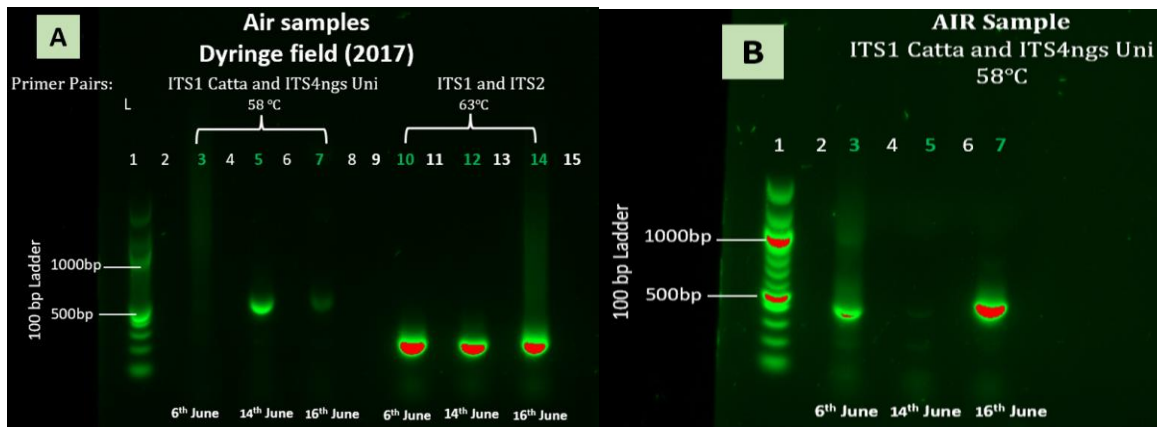
Appendix 6. Gel displays PCR-amplified products, which were run using two different primer pairs and temperatures for optimizing temperature for specific primer pairs. A) Demonstrates PCR-amplified products run at different gradient temperatures 61°C to 65°C on leaf samples collected from Skofteby field, using primer pair ITS1 and ITS2. B) Shows PCR-amplified products run at different gradient temperatures 58°C to 63°C on leaf samples collected from Skofteby field, using primer pair ITS1 Catta and ITS4ngs Uni.



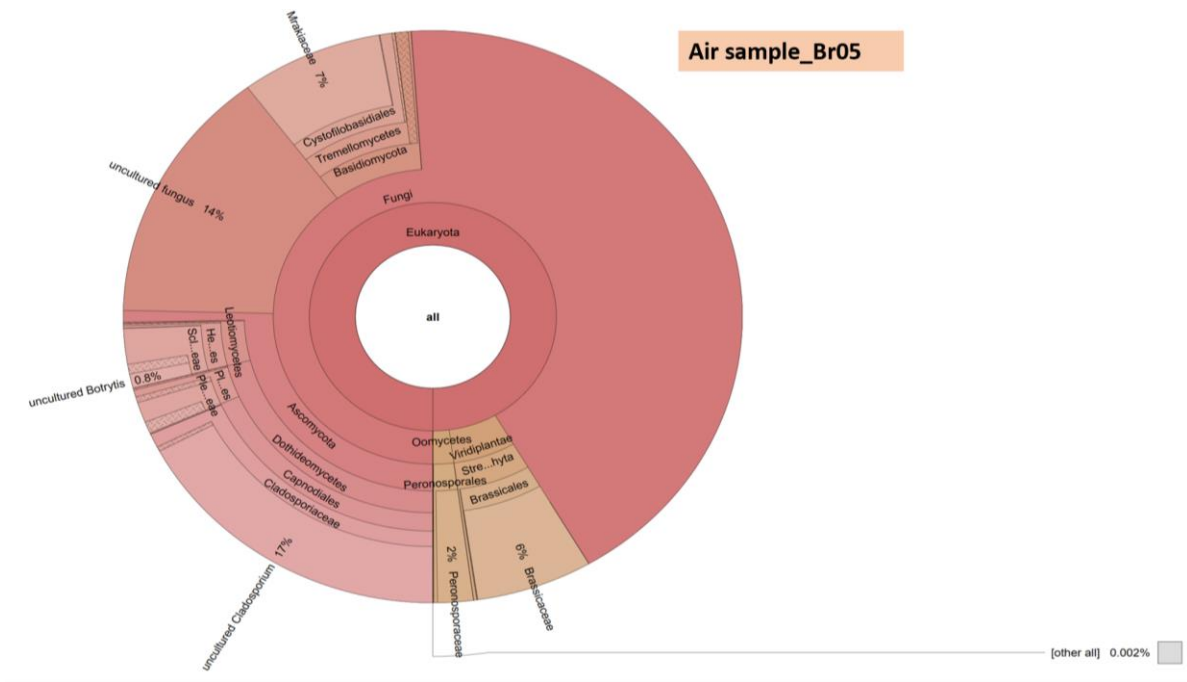
Appendix 7. Gel displays PCR-amplified products, which were run using two different primer pairs and temperatures. A) Shows PCR-amplified products run at an annealing temperature 58°C on leaf samples collected from Skofteby, Forsby and Kaflas fields, using primer pair ITS1 Catta and ITS4ngs Uni. B) Demonstrates PCR-amplified products run at an annealing temperature 63°C on leaf samples collected from Skofteby, Forsby and Kaflas fields, using primer pair ITS1 and ITS2.



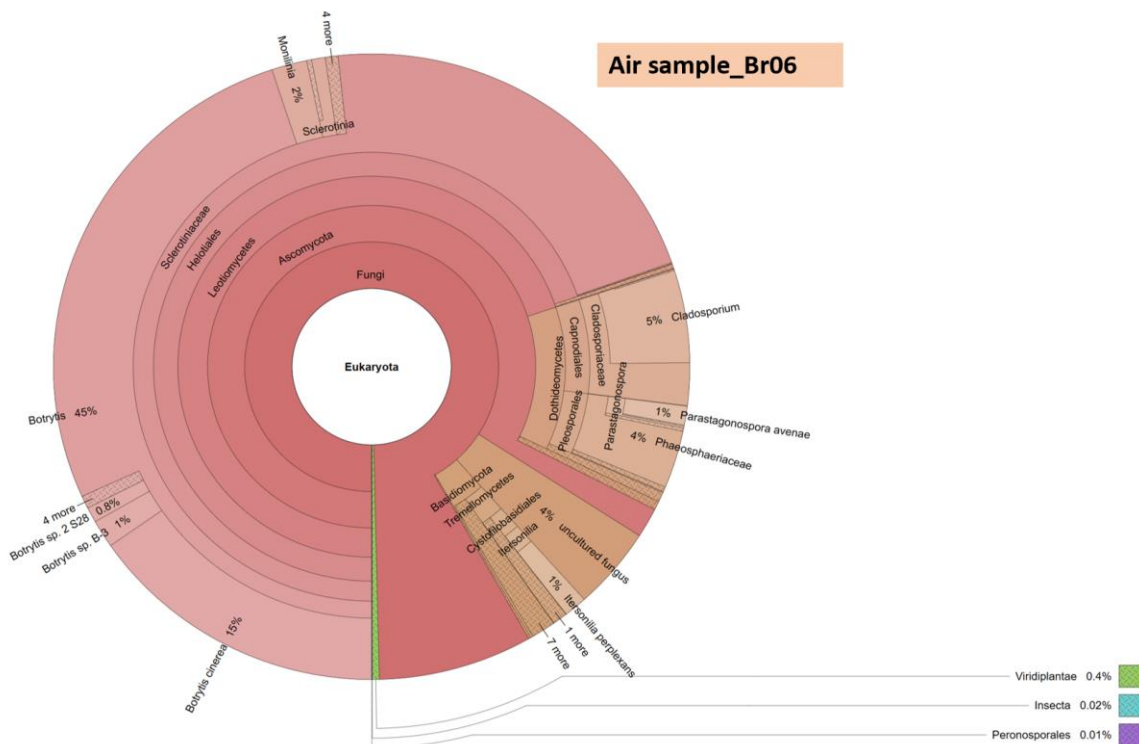
Appendix 8. Gel displays PCR-amplified products, which were run using two different primer pairs and temperatures. A) Shows PCR-amplified products run at an annealing temperature 58°C on soil samples collected from Forsby and Keflas fields, using primer pair ITS1 Catta and ITS4ngs Uni. B) Demonstrates PCR-amplified products run at an annealing temperature 63°C on soil samples collected from Forsby and Keflas fields, using primer pair ITS1 and ITS2.



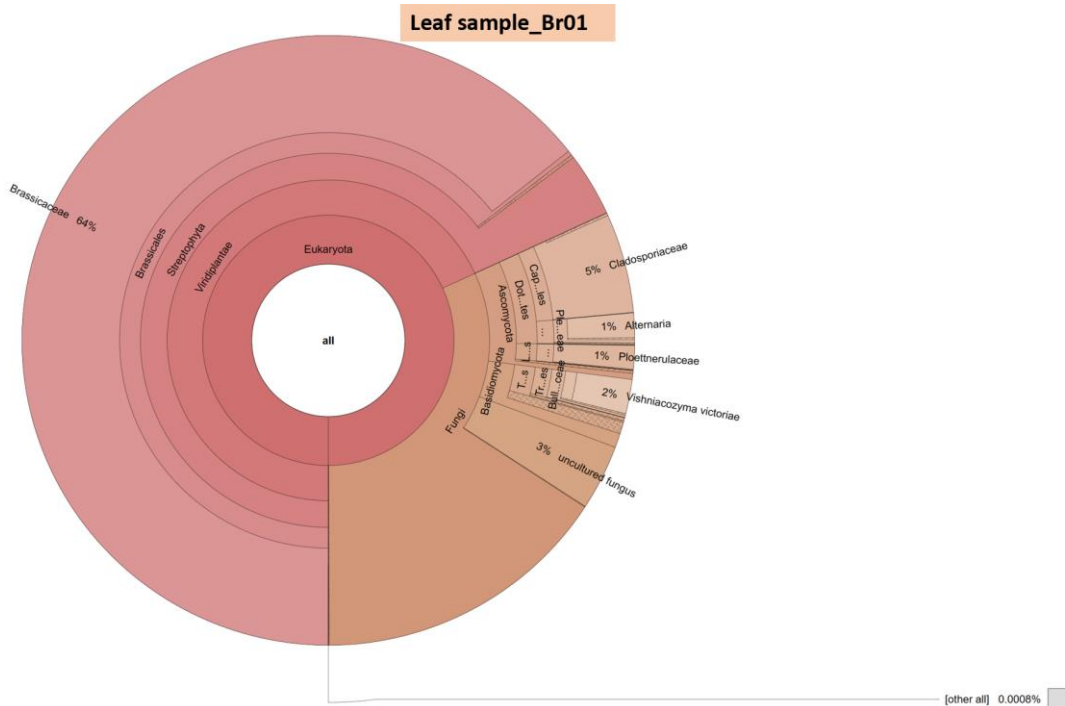
Appendix 9: A) Gel displaying PCR-amplified products run using two different primer pairs and temperature. The primer pair ITS1 Catta and ITS4ngs Uni was used for samples in lanes 3,5, and 7, with an annealing temperature of 58°C. For the primer pair ITS1 and, the annealing temperature was 63°C, and samples were run in lane 10,12, and 14. These samples comprised air samples collected on June 6th, 14th, and 16th 2017. B) Gel showing PCR-amplified products run on the annealing temperature 58°C for sample extracted on dates: 6th, 14th, & 16th June 2017, from Dyringe fields (air samples), using ITS1 Catta and ITS4ngs Uni.



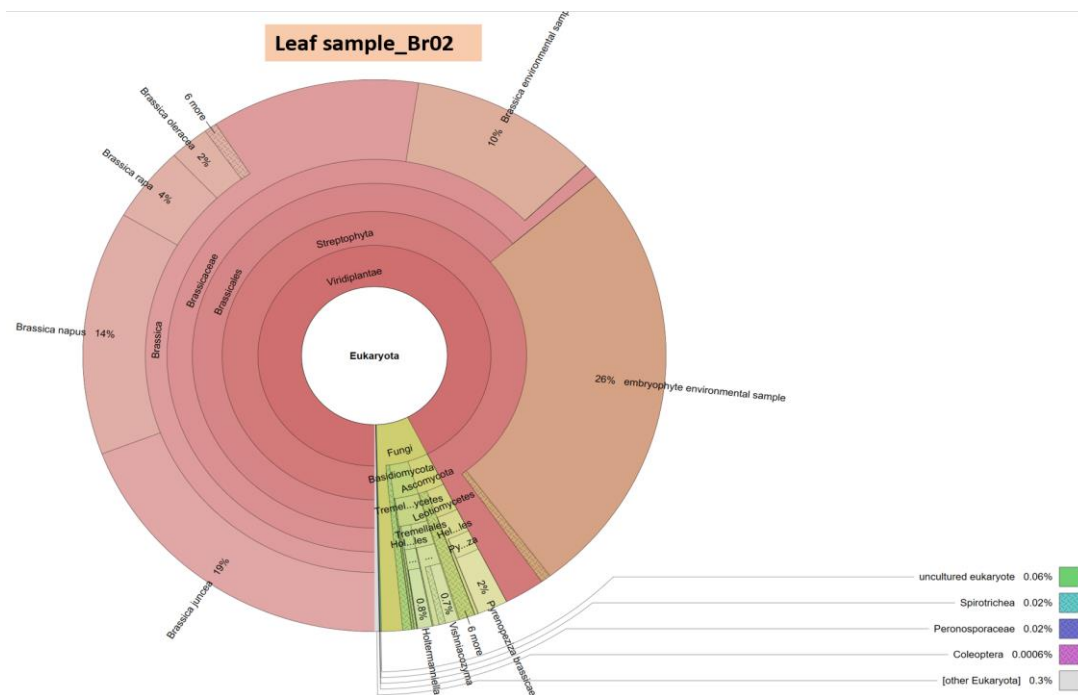
Appendix 10: A full screenshot of the krona plot produced by CCMetagen for 16th June 2017, air sample. Amplified by using primer pair ITS1-ITS2 and spiked with gDNA of *S. sclerotiorum* displaying the presence of *S. sclerotiorum* at level of 63%.



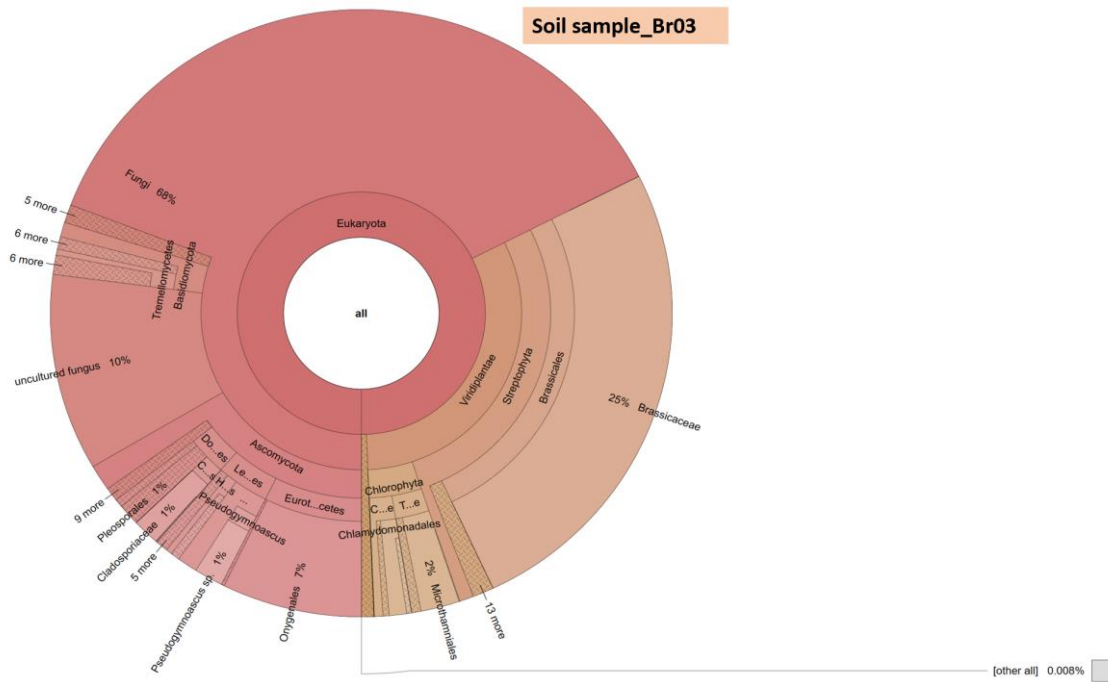
Appendix 11. A full screenshot of krona plot produced by CCMetagen for 14th June 2017, air sample. Amplified by using the primer pair ITS1Catta-ITS4ngs Uni. Displaying the presence *S. sclerotiorum* at level of 12%.



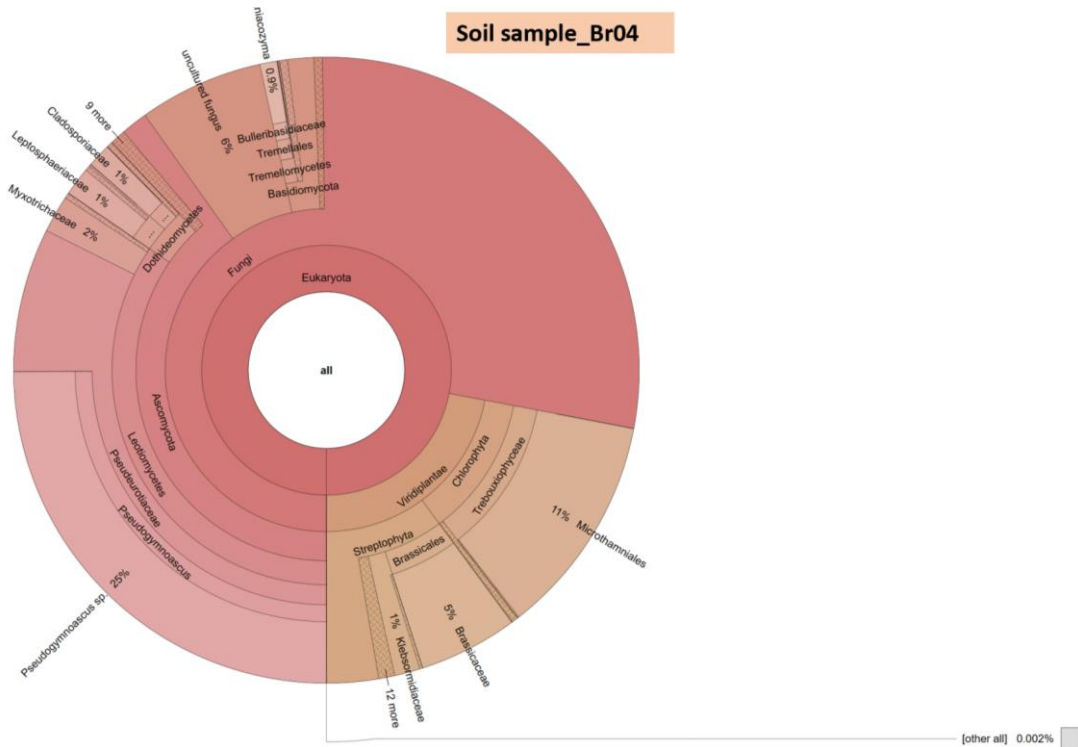
Appendix 12: A screenshot of the krona plot produced by CCMetagen for a pooled leaf sample from Kafkas field. Amplified using primer pair ITS1-ITS2 and revealed that no *S. sclerotiorum* was observed, but other pathogens were detected.



Appendix 13: A screenshot of the krona plot produced by CCMetagen for a pooled leaf sample from Skofteby field. Amplified by using primer pair ITS1Catta-ITS4ngs Uni and revealed that no *S. sclerotiorum* was observed, but other pathogens were detected.



Appendix 14: A screenshot of the krona plot produced by CCMetagen Forsby soil field. Amplified by primer pair ITS1-ITS2 and revealed that no *S. sclerotiorum* was observed, but other pathogens were detected.



Appendix 15: A screenshot of the krona plot produced by CCMetagen for Kaflas soil field. Amplified by using primer pair ITS1-ITS2 and revealed that no *S. sclerotiorum* was observed, but other pathogens were detected.

Appendix 16. Presenting list of fungi causing damages to oilseed rape plant with respect to its percentage found in different samples.

| Fungi | Samples | Percentage (%) |
|-------------------------------|--|-----------------------|
| <i>Alternaria alternata</i> | Skofteby (pooled leaf) | 2 |
| | Dyringe (air:14 th June 2017) | 88 |
| <i>Alternaria infectoria</i> | Skofteby (pooled leaf) | 83 |
| <i>Botrytis cinerea</i> | Kaflas (pooled leaf) | 43 |
| | Dyringe (air:14 th June 2017) | 15 |
| <i>Pyrenopeziza brassicae</i> | Skofteby (pooled leaf) | 2 |
| <i>Phytophthora</i> | Forsby (soil) | 12 |
| <i>Pythium</i> | Forsby (soil) | 2 |